63-3-5

405769

ASD-TDR-63-16

The Photoelectric Rotating Slit Elevation and Azimuth Sensor (PERSEAS)

ASD Technical Documentary Report No. ASD-TDR-63-16

MARCH 1963 • AFSC Project No. 7844

DIRECTORATE OF ARMAMENT DEVELOPMENT

Det 4, AERONAUTICAL SYSTEMS DIVISION

AIR FORCE SYSTEMS COMMAND • UNITED STATES AIR FORCE

EGLIN AIR FORCE BASE, FLORIDA

(Prepared under Contract No. AF 08(635)-2631 by Military Physics Research Laboratory, The University of Texas, Austin, Texas. Herman E. Brown and Mark D. Glasgow, authors.)

ASD-TDR-63-16
MPRL 552

THE PHOTOELECTRIC ROTATING SLIT ELEVATION AND AZIMUTH SENSOR (PERSEAS)

March 1963

AFSC Project No. 7844

FOREWORD

In January of 1962 this Laboratory accepted study Contract AF 08(635)-2631 with the Applied Research Branch, Target Development Laboratory, Det 4, ASD at the Air Proving Ground Center, Eglin Air Force Base, Florida, for the prime purpose of studying physical phenomena which are promising for the development of scoring devices. As an outgrowth of this contract a supplemental agreement was added to the statement of work which provided for a feasibility study of a coordinate sensing device that could possibly be developed into a scoring system. Two sensing devices were constructed for laboratory studies. The first, known as the Photopot System did not prove feasible; the second device, known as PERSEAS is considered a feasible concept.

I would like to express my gratitude to Mr. Vito Marinelli of the Applied Research Branch, Target Development Laboratory whose suggestions and criticisms of these scoring concepts were most valuable.

Herman E. Brown
Research Scientist Associate V

Catalog cards may be found in the back of this document.

ABSTRACT

A description is presented of

~~This report described~~ a laboratory experimental study of two optical sensing devices which appeared to be worthy of feasibility studies for the specific development of scoring devices. The first device, known as the Photopot System, did not prove feasible as a useful sensor~~because of its slow response and low sensitivity~~. The second device, known as PERSEAS is considered appropriate for further development. Studies have shown that PERSEAS is highly accurate for the measurement of relative azimuth and elevation angles, and studies of the concept have so far revealed no major limitation which would prevent development of a complete scoring system.

PUBLICATION REVIEW

This technical documentary report has been reviewed and is approved.

L. S. KARABLY
Lt Colonel, USAF
Chief, Target Development Laboratory

TABLE OF CONTENTS

TABLE OF CONTENTS

THE PHOTOELECTRIC ROTATING SLIT ELEVATION AND AZIMUTH SENSOR (PERSEAS)

I. INTRODUCTION

In January of 1962 the Military Physics Research Laboratory of The University of Texas began work on Contract AF 08(635)-2631 which provided for a study of physical phenomena and techniques which could be instrumented for the development of scoring devices. The study encompassed all phenomena such as magnetic field, gravitational fields, electromagnetic radiation and shock waves.

As an outgrowth of the study it became evident that the optical portion of the electromagnetic spectrum offered several advantages for the development of a scoring device. A good many optical sensors were studied during the investigations of the optical wave lengths, and some of them were considered worthy of experimental studies. They included phototransistors, photopotentiometers, image orthicons, and photomultiplier tubes. All of these devices offered common advantages and they could be easily instrumented for the measurement of relative azimuth and elevation angles of a light source. These advantages are:

1. No requirement to measure signal frequency
2. No requirement to measure signal phase
3. No requirement to measure signal amplitude
4. Simple electronic circuits

A supplemental agreement to the contract called for experimental studies of optical devices. The Photopot sensor (manufactured by Giannini Controls Corporation) was instrumented for angular measurements but it proved to be too insensitive for the scoring problem. It also has a long response time. A system called PERSEAS (Photoelectric Rotating Slit Elevation and Azimuth Sensor) was designed following the Photopot experiments, and it has proved quite successful. The majority of this report is concerned with studies of the PERSEAS system.

II. EXPERIMENTAL STUDIES OF THE PHOTOPOT SYSTEM

Introduction. - A Photopot is a device which senses a point source of light at some range R; the output voltage of the device is proportional to the azimuth or elevation coordinates of the source depending upon the orientation of the Photopot. The device consists of a light-actuated semiconductor analog of the mechanically operated potentiometer. It is basically a photoconductive crystal containing parallel deposits of a resistive strip and a non-sensitive collector. Voltage is divided by light falling upon the photoconductive gap.

In the studies that were planned for the Photopot to determine its usefulness as a sensor for a scoring device, a cylindrical lens was to be used with the Photopot to project a line image of the light source on the photoconductive gap. Experiments conducted in the Laboratory with the Photopot proved beyond doubt that the device did not have the response or sensitivity required for the scoring problem and as a result the device was abandoned for studies which led to the PERSEAS system. Nevertheless this chapter of this report is concerned with the studies which were conducted with the Photopot.

Photopot System Design. - The optical sensing device described here represents one component of a scoring system. The device should sense a point source of light at some range R, and the voltage outputs of the device should be proportional to the azimuth and elevation angles of the line-of-sight in the coordinate system associated with the vehicle containing the angle-sensing device. A second device placed at some suitable distance from the first device along a base line should produce a set of voltages proportional to its line-of-sight angles in azimuth and elevation. The two sets of angles, along with the base line, could be used to compute a range by the triangulation method.

Since this was a feasibility study, only one device was constructed and tested. If the test had shown the device to represent a suitable technique for measuring angles to the accuracy required in a two-station system, feasibility would have been proven.

The sensing elements used in the device were photopotentiometers, one of which is illustrated in Figure 1. Each photopotentiometer was to be used in combination with a cylindrical lens arranged as shown in Figure 2, two such combinations comprising one device. The arrangement of the overall combination is shown in Figure 3. Each photopotentiometer and lens combination was to be associated with a plane containing the light source, with the intersection of the two planes representing the line-of-sight. The field of view would be determined by the active length of the photopotentiometer and the focal length of the lens.

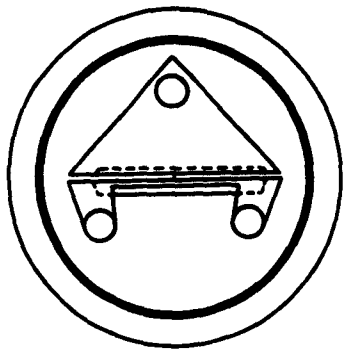

Figure 1. Photopot

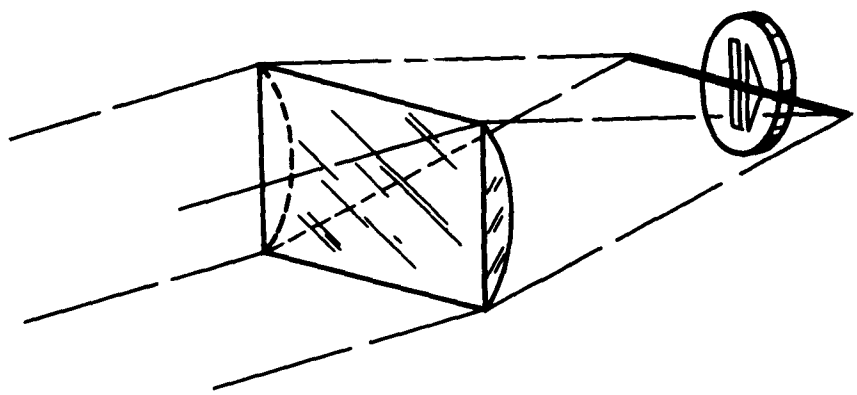

Figure 2. Photopot and Cylindrical Lens

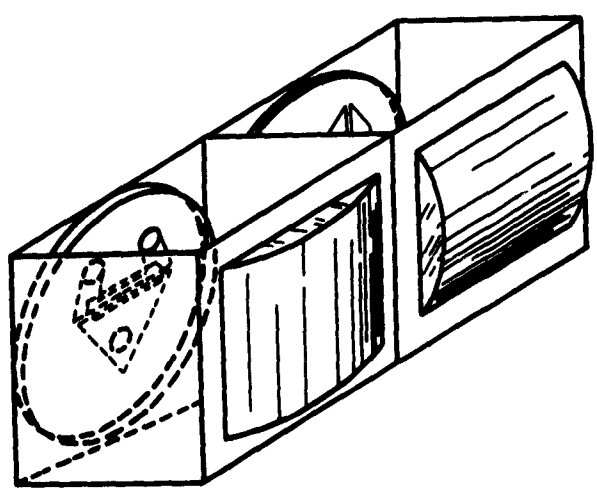

Figure 3. Single Station Configuration

Some other considerations of importance in the selection of a lens-photopotentiometer combination are discussed in the paragraphs to follow.

The light power intercepted by a cylindrical lens is

$$P_\ell = P_o A_\ell$$

where P_o = power density in the vicinity of the lens and A_ℓ = area of lens (product of length and aperture width). The power density (intensity) in the focused line image is the total power collected by the lens divided by the area of the image, A_i, over which the collected power is distributed. The foregoing assumes, of course, a uniform distribution in the image. It is recognized that such uniformity in the image is not a good approximation. The results obtained, however, should be conservative because of the assumption. That is, the intensity computed for the image should actually be greater at its center than at the edges, and therefore greater at the center than predicted by assuming a mean value all across the image.

The length, ℓ, of the line image formed by a cylindrical lens should be the same as that of the lens. The width, d, of the image would be determined by diffraction effects (assuming a point source of light and a perfect lens) and this value is given by,

$$d = \frac{\lambda}{a} f$$

where λ is the wavelength of the light being used, a is the aperture width of the cylindrical lens, and f is its focal length.

The power density in the image is

$$P_i = \frac{P_\ell}{A_i} = \frac{P_o A_\ell}{A_i}$$

$$= P_o \frac{\ell a}{\ell d}$$

$$= P_o \frac{a}{d}$$

$$= P_o \frac{a}{(\lambda/a) f}$$

or

$$P_i = P_o \frac{a^2}{\lambda f} = P_o \frac{a}{\lambda f} a = P_o \frac{1}{\lambda F'} a$$

where F' is the "f-number" which is the ratio (f/a). The important feature of this relation which should be noted is that the intensity in the image varies directly as the square of the lens aperture width but inversely only as the first power of the lens focal length. For illustration of the significance of this fact, the image intensity can be increased directly as "a" by increasing "a" and at the same time by letting the focal length increase proportionally. That is, if the f-number or f-ratio, f/a, is a measure of the lens "speed," just as with spherical lenses, then the situation could be bettered by making the lens larger (greater aperture width) without demanding greater lens "speed."

As the lens aperture is increased to increase image intensity while maintaining the same f-ratio, a given linear motion of the image in the focal plane would represent a progressively smaller field-of-view. For a photosensitive element such as the Photopot, which has an upper limit on the length available, there obviously has to be some trade-off or compromise between image intensity and the field-of-view. These were the considerations which led to the initial Photopot-lens designs presented at this time.

At the time the proposal was written for this study, the available literature indicated that photopotentiometers with an active length of one inch could be obtained as off-the-shelf items. Since then, however, it has been learned that the longest available length in production models of the Photopot is approximately 0.3 inch.

To compensate for the effects resulting from the use of a sensing element of shorter length, two choices were available:

1) The same field of view could be mainteined by using a shorter focal-length lens such as the linear motion of the light-source image, for light-source motion across the entire field-of-view desired is equal to the length of the photosensitive element available (0.3 in.)

2) The field-of-view could be scaled down proportional to the factor by which the sensing element is shorter than was originally planned.

The latter choice was made, principally because this choice would allow the use of longer focal-length lenses and larger apertures, subsequently providing higher light intensities in the image.

As was pointed out, this choice forced a reduction in the field-of-view. Such a reduction in the field-of-view was not, however, so great as to prevent testing the feasibility of the concept, and had the feasibility experiments proved successful, the full field-of-view originally intended could be had by specially designed Photopots somewhat longer than those currently available. Giannini Controls Corporation indicated that it could supply one-inch Photopots.

Three different lens-Photopot-holder designs were provided, together with design of the three different lens sets with which they were to be used. The design made it possible to maintain the same aperture size while changing the "f-number" by varying the focal length rather than holding the field-of-view constant while increasing the aperture to give various intensities. This decision also permitted simpler construction procedures. The particular combinations chosen are tabulated below.

TABLE I

LENS CHARACTERISTICS

lens aperture (inches) (a)	f-number $F' = \frac{f}{a}$	focal length (inches) (f)	Photopot sensitive element length (inches)	total field-of-view (degrees)
2.25	1.0	2.25	0.3	7.64
2.25	1.2	2.70	0.3	6.36
2.25	1.4	3.15	0.3	5.47
2.25	1.0	2.25	1.0	25.07
2.25	1.2	2.70	1.0	11.00
2.25	1.4	3.15	1.0	18.07

The light source used was a compact Xenon arc lamp. This lamp was chosen because its output is very close to that of a black-body radiator, and it is a more efficient light source than a filament type source. The arc is small and may be used to approximate an intense point source, which will be imaged as a line by a cylindrical lens.

Failures of the Photopot System. - The experimental studies for the Photopot were not conducted as planned, primarily because of delay in delivery of the cylindrical lenses. However, a revised experimental program was undertaken using an available spherical lens to determine the dynamic response of the Photopot. This program was successful beyond doubt in showing that the Photopot did not have the dynamic response required for the scoring problem. In addition,

the experimental program showed that the Photopot was far too insensitive to be a useful optical sensor for light sources below 1000 watts input power.

Several experiments were conducted on the Photopot pending receipt of the cylindrical lenses. These experiments were directed towards determining the Photopot dynamic response when subjected to a very intense light source. In general, the results of these studies were discouraging and they led to the conclusion that the Photopot did not have the required response.

In these experiments, the Photopot was mounted on a rotating plate and centered about 3/4" from the center of rotation (see Figure 4). The Photopot was aligned so that the sensitive element was in effect a segment of a radius of the rotating plate. A high quality F/1.9, 75 mm spherical lens was mounted parallel to the rotating plate, centered on the rotation axis, and carefully adjusted so that the sensitive element of the Photopot was in the focal plane of the lens. A variable-speed motor was used to drive the rotating plate and a strobotac was used to measure the angular rate.

The Photopot output was connected to the vertical deflection plates of a cathode ray oscilloscope and also to the horizontal sweep trigger. In this way a signal produced by the Photopot initiated a horizontal sweep of the oscilloscope trace and also deflected the trace vertically proportional to the output amplitude. The resultant effect was a plot on the CRT face of the Photopot output vs time. Photographs of some of the results, which are reproduced in Figures 5-a, 5-b, and 5-c, were taken for several rotational speeds. The response time and output amplitude were determined from the photographs. Although the reproductions of the photos are not very clear, they are included to show the form of the original data taken.

The peak amplitude as a function of rotational speed was measured for each speed at which the Photopot was rotated where one exposure occurred for each resolution. The results are presented in Figure 6 in the form of a plot of the peak output amplitude versus the exposure rate. Since one component of the light source coordinates is proportional to output voltage, the output voltage should not vary with the speed at which the Photopot is rotated until the response time is exceeded.

The light source for this data was a 1000-watt Xenon lamp placed at a distance of 43 feet from the lens. The spot size was measured to be 0.018" and the electrical width of the sensitive element was measured to be 0.005" on the average. It is believed that the electrical width varies with spot size. This was not verified by careful measurements, however.

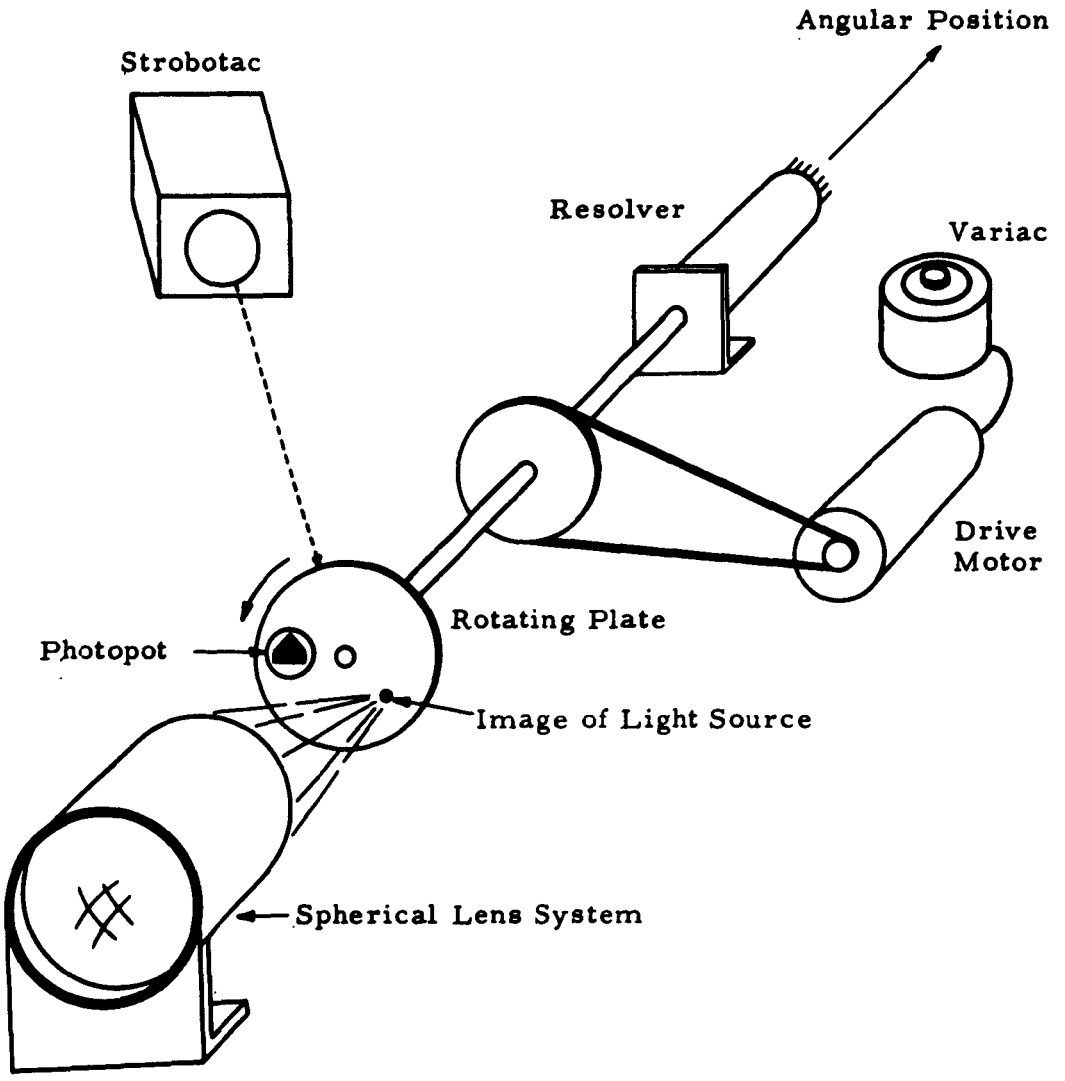

Figure 4

Experimental Configuration for Response Measurements

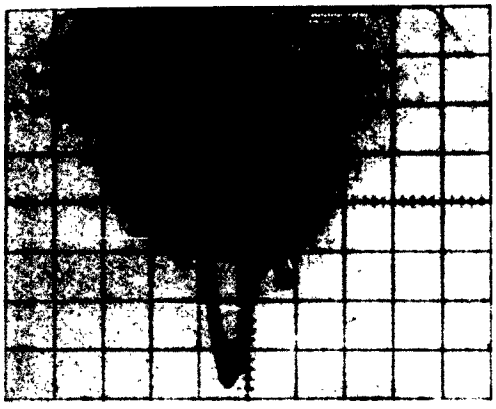

Speed = 125 RPM
Spot Size = .018"

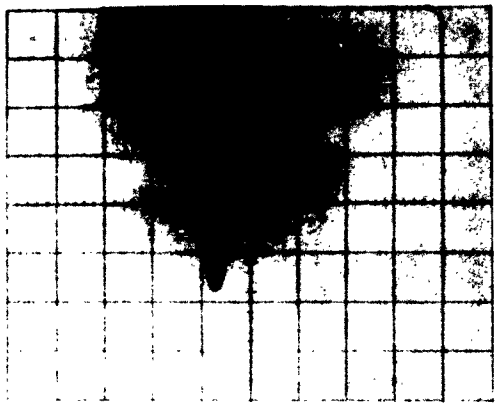

(2) Speed = 300 RPM
Spot Size = .018"

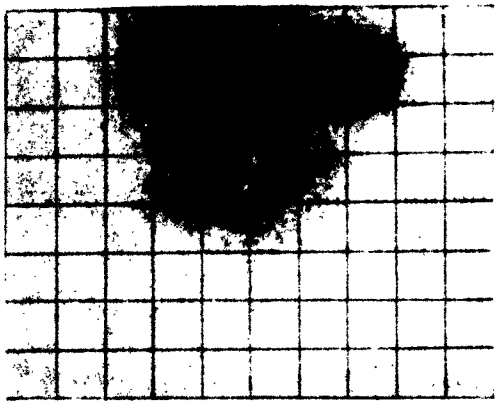

(3) Speed = 375 RPM
Spot Size = .018"

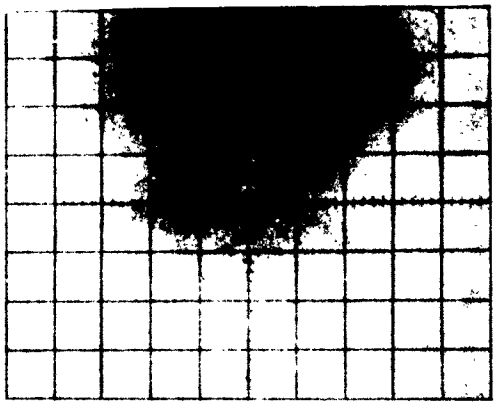

(4) Speed = 490 RPM
Spot Size = .018"

Figure 5-a

Photopot Output versus Time

(5) Speed = 650 RPM
Spot Size = 018"

(6) Speed = 750 RPM
Spot Size = 018"

(7) Speed = 875 RPM
Spot Size = .018"

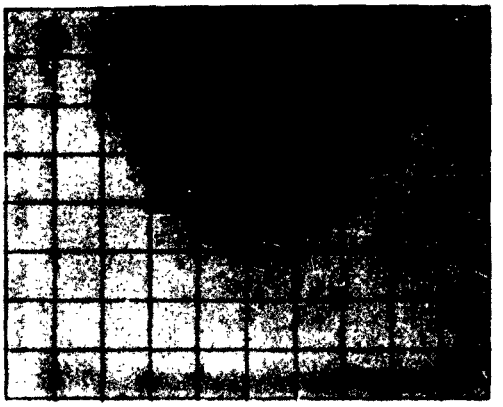

(8) Speed = 970 RPM
Spot Size = .018"

Figure 5-b

Photopot Output versus Time

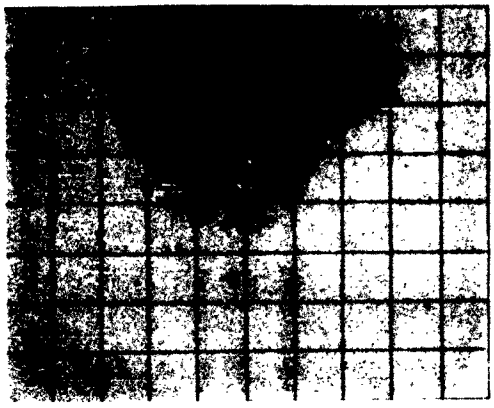

(9) Speed = 1060 RPM
Spot Size = .018"

(10) Speed = 1200 RPM
Spot Size = .018"

Figure 5-c

Photopot Output versus Time

The radial distance of the spot from the center of rotation for all of the data was 26/32"; therefore the angle subtended at the rotation axis by the spot was

$$\theta_s = \frac{D_s}{R} = \frac{0.018}{26/32''} \simeq 0.022 \text{ radian}$$

and the angle subtended by the sensitive element for this radius was

$$\theta_E = \frac{D_E}{R} = \frac{0.005''}{26/32''} \simeq 0.00625 \text{ radian}$$

The difference of these two angles (0.016) then is the angular motion that occurs over the time interval during which the sensitive element is completely exposed. The exposure time will be

$$t = \frac{0.016}{2\pi f} \text{ min}$$

where f is the number of exposures per minute or speed of the rotating plate in rpm. The exposure time for each constant angular rate has been calculated and also plotted in Figure 6. This shows that output voltage is a direct function of exposure time, and this cannot be tolerated in this scoring concept.

The horizontal time scale on the photographs is about 400 microseconds per division. It may be seen that none of the pulses reach a constant amplitude even for the lowest rotational speed. This fact shows that the sensitive element does not have sufficient time to reach saturation during the exposure interval. Measurements at lower speeds determined the minimum exposure time for complete saturation to be about 900 microseconds.

These experiments were conclusive regarding use of a Photopot as a sensor. It was not considered necessary to duplicate the results with cylincrical lenses.

Conclusions and Decisions Concerning the Photopot System. - Although the experimental studies proposed for the Photopot were not carried out as planned, sufficient response information was obtained to conclude that the Photopot could not be used as a sensor in a scoring device. This conclusion was reached primarily because of the very long response time of the device. For satellite scoring where the entire time interval of the intercept may be in the order of 40 to 50 milliseconds, a sensor which requires one millisecond steady state conditions to provide a readout cannot be used. In summary, the

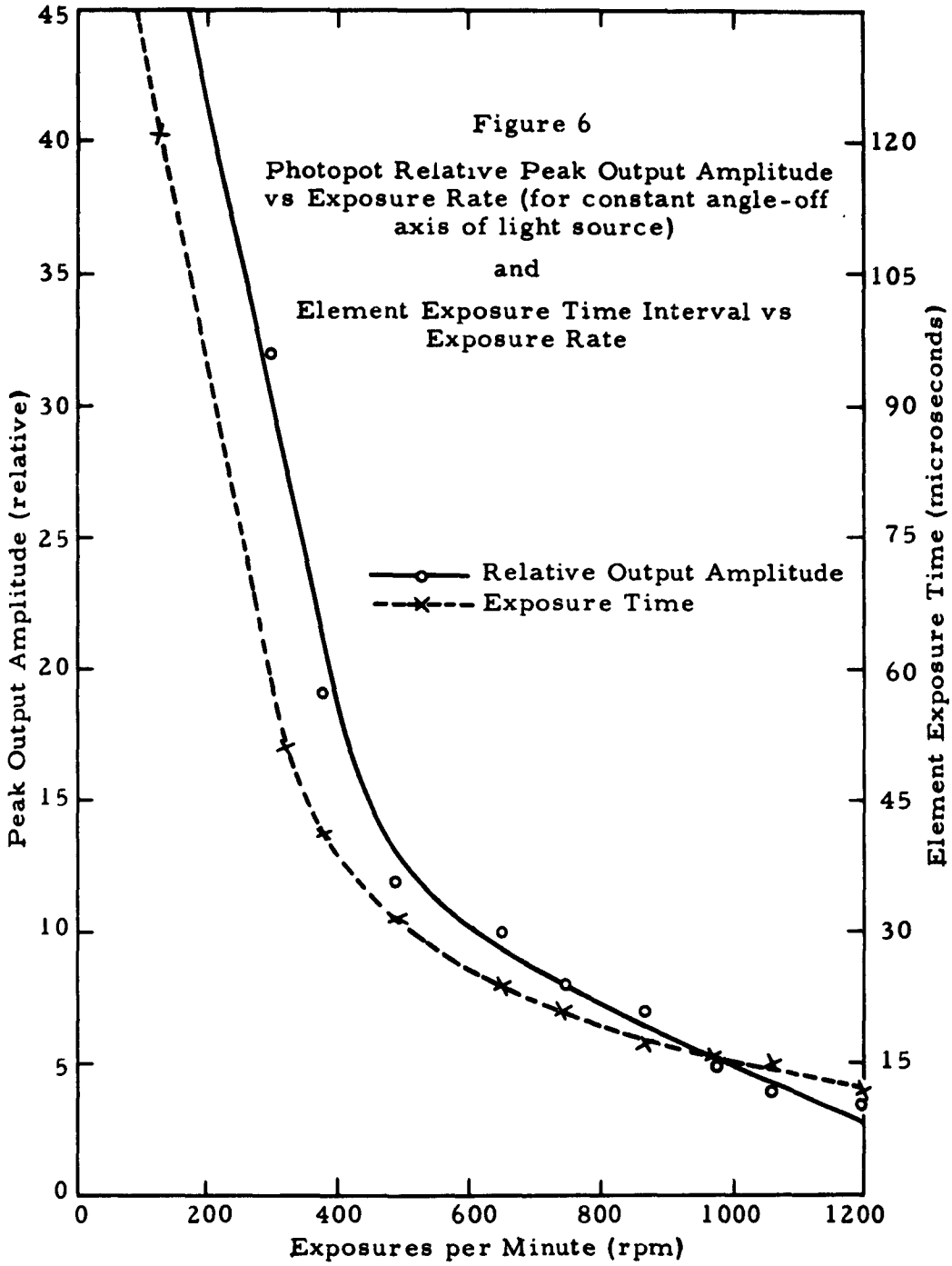

Figure 6

Photopot Relative Peak Output Amplitude vs Exposure Rate (for constant angle-off axis of light source)

and

Element Exposure Time Interval vs Exposure Rate

following characteristics of the Photopot rule it out as a good sensor:

1. Response time is far too long.
2. Sensitivity is far too low.

Since these conclusions were reached rather early in the experimental program, it was necessary to make decisions concerning the remainder of the work. It was decided to abandon the Photopot concept and continue with another concept that might prove worthwhile as a scoring sensor. Several other concepts had been generated in the Laboratory, one of which concerned a device consisting of a photomultiplier as the sensor and a system of rotating slits to measure the coordinates of the light spot. It was decided to explore this concept, and the remainder of the effort was directed toward a study of a device embodying this concept.

III. DESIGN OF THE PHOTOELECTRIC ROTATING SLIT ELEVATION AND AZIMUTH SENSOR

After it was concluded that the Photopot system was not feasible for the design of a scoring device, it was decided to direct efforts toward another concept which appeared to be promising as a potential scoring device. The remainder of this report is concerned primarily with the design and experimental studies of the Photoelectric Rotating Slit Elevation and Azimuth Sensor. This device will be referred to as PERSEAS.

Many sensors operate in the optical region of the electromagnetic spectrum. In reviewing the character of the optical sensors with primary consideration being placed on sensitivity and response time, it was decided that the photomultiplier tube is very promising as the sensing element of a scoring system. There are some recognized disadvantages of the photomultiplier, namely size, physical configuration, and the requirement of high excitation voltages. These disadvantages were not considered serious; that is to say, with good engineering design, it is possible to work around the recognized disadvantages.

After having concluded that the optical portion of the spectrum offers many advantages for the design of a scoring device, it was decided that a simple device could be fabricated which would take advantage of the high sensitivity and response time of the photomultiplier tube. The design was carried out with off-the-shelf items, and for this reason the optics of the system are not of the best design. Nevertheless, off-the-shelf items were good enough for the experimental study.

The device embodying this concept (see Figure 7) involves the use of a spherical lens, a prism, a photomultiplier tube, and a rotating section of a sphere which has very narrow slits at equal intervals around the spherical section. The purpose of the slits is to pass the light image into the photomultiplier when the slit and image are coincident. The coordinates of the image of a distant point source in the focal plane of the lens will be linearly related to the actual relative coordinates of the source. As the slit passes over the spot image, it passes the light to the photomultiplier and a pulse is produced. Through timing or some means of measuring the angle of the slit at the instant the pulse is produced, a direct instantaneous measure of the spot coordinate is obtained. The focal plane of the lens will have the same general shape as the inner surface of the rotating spherical section. Therefore, when a slit is in the field of view, it is in the focal plane of the lens. The only function of the prism is to reverse the direction of the light rays; however, in doing so, the effective focal length of the lens is increased.

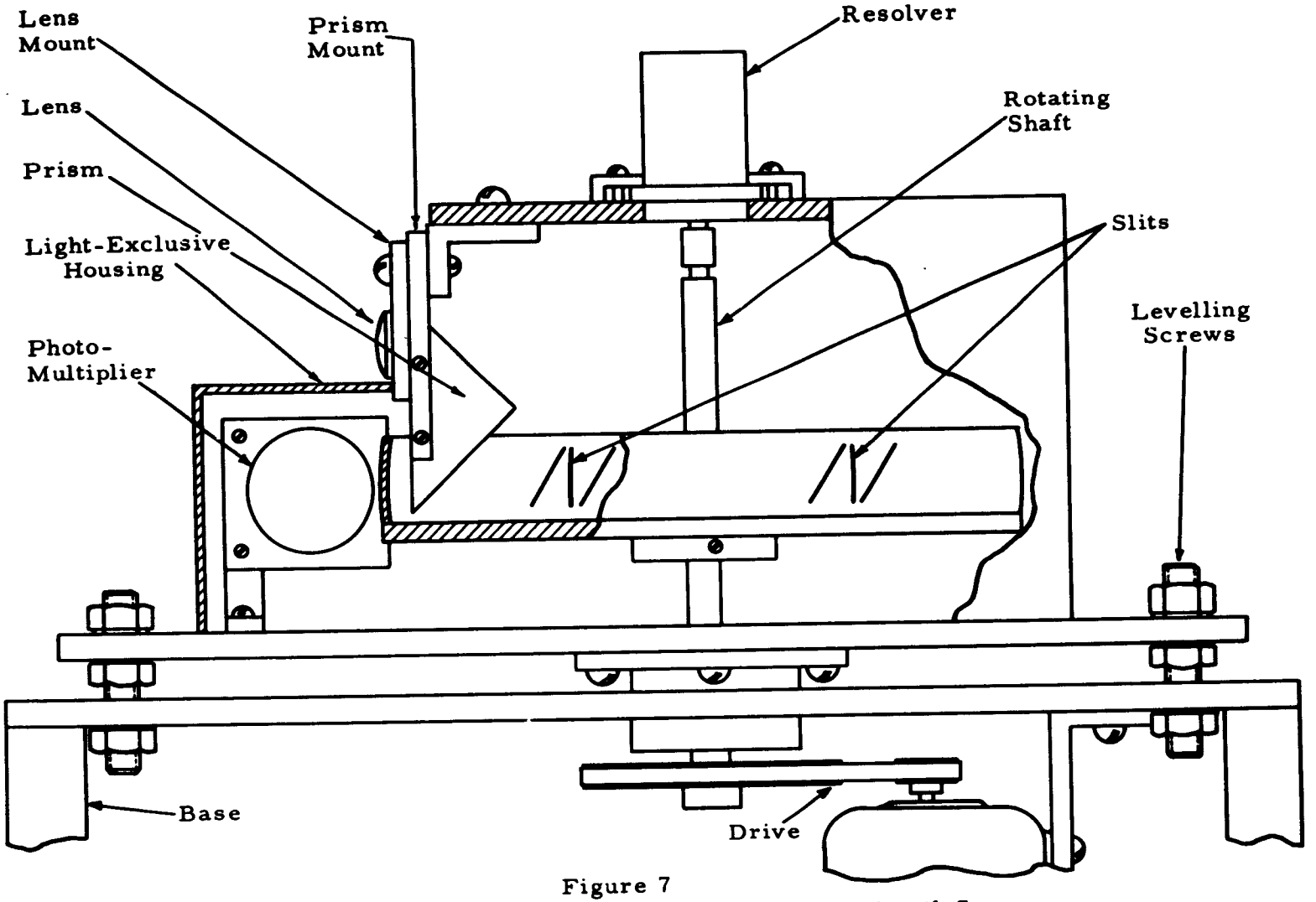

Figure 7
Photo-Electric Rotating Slit Elevation and Azimuth Sensor

Design Parameters

The basic design for the PERSEAS was initially carried out for obtaining only azimuth coordinates of the light source. The following assumptions were made in carrying out the design:

1. Radius of the rotating spherical section will be 3 inches.
2. Focal length of the lens prism system will be 3 inches.
3. Angular coverage of a single lens, prism, and photomultiplier combination should be about 45°.
4. The minimum time for a scoring intercept should be 40 milliseconds.
5. A minimum of 10 data points will be required to reconstruct a relative path of the light source.

For 360° coverage and 45° per unit it is seen that

$$\frac{360^{\circ}}{45^{\circ}/\text{unit}} = 8 \text{ units}$$

Thus 8 azimuth slits at equally spaced intervals are required around the drum.

The minimum drum velocity may be determined as

$$\frac{\frac{10 \text{ points}}{8 \text{ points/rev}}}{40 \text{ M sec} \times 10^{-3} \frac{\text{sec}}{\text{M sec}} \times \frac{1 \text{ min}}{60 \text{ sec}}} \simeq 1900 \text{ rpm}$$

Since 1800-rpm motors (synchronous type) are common, it was decided to use this type. A 3600-rpm motor could also be used and provide twice as many data points.

Angular resolution is considered a function of the slit width.

$$\text{Drum circumference} = 2\pi R \simeq 18.8''$$

$$45^{\circ} \text{ arc length} = \frac{18.8''}{8} \simeq 2.35''$$

For 1 mil resolution

$$\text{Slit width} = \frac{\text{arc length}}{800 \text{ mils}} = \frac{2.35''}{800} \simeq 0.003''$$

The smallest saw available was 0.004" so it was used to cut the slits.

Sensitivity calculations are based on a type 931A photomultiplier tube (see Reference 2) that will produce 30,000 microamps per microwatt input power. A maximum distance of 2000 ft is assumed for calculations.

$$\text{Power Density} = \frac{P_o}{4\pi R^2}$$

$$= \frac{P_o}{4\pi(2000)^2} \frac{\text{watts}}{\text{ft}^2}$$

where R is range in ft between the source and the collecting lens and P_o is the total radiated power.

Assume the lens is 1" in diameter

$$\text{Lens area} = \pi r^2 = \frac{\pi \text{ in}^2}{4} \times \frac{1 \text{ ft}^2}{144 \text{ in.}^2}$$

$$= \frac{\pi}{4(144)} \text{ ft}^2$$

$$\text{Power at lens} = \frac{P_o \pi}{4\pi(2000)^2 \, 4(144)} \text{ watts}$$

$$\simeq 10^{-10} \, P_o \text{ watts}$$

Assume a minimum signal requirement of 100 millivolts and a load resistance of 10^5 ohms

$$\text{Current I} = \frac{0.1 \text{ volts}}{10^5 \text{ ohms}}$$

$$= 10^{-6} \text{ amps} = 1 \text{ microamp}$$

Since the photomultiplier will produce 30,000 microamps per microwatt, the input power to the tube for 1 microamp output must be,

$$\text{Total input power} = \frac{1 \text{ microamp}}{30,000 \text{ microamps/microwatt}}$$

$$\simeq 3.3 \times 10^{-11} \text{ watts}$$

From this it is seen that the minimum power radiated at the source (P_o) must be

$$\text{Power at Lens} \simeq 10^{-10} P_o$$

$$P_o \simeq \frac{3.3 \times 10^{-11}}{10^{-10}} = 0.33 \text{ watt}$$

In practice this is not a realistic figure for the power because noise signals have not been considered. A source with considerably more power should be used.

It would not be possible to operate the system in an environment where there is an intense amount of light such as outside during the day or in a lighted room. The tube has such a large amplification that it will become saturated with very little light. Of the several ways of limiting the amount of light entering the lens, the two most promising are:

1. Use of interference filters for selecting only a narrow band of wavelengths
2. Use of a polarized light source and filter to permit only selected polarized light to pass to the photomultiplier.

Of these two methods, only (1) has been used.

Addition of the Elevation Slits. - The original concept for this system provided for the measurement of only one angular coordinate, say azimuth, of a light source. Initial configuration of the drum provided for only 8 azimuth slits equally spaced around the drum. After initial success was demonstrated with the system for measuring azimuth coordinates, a technique was devised for adding the capability of elevation coordinate measurements. This technique consists of adding a slit on each side of the azimuth slits at a 45 degree angle relative to the azimuth slit. The two elevation slits are parallel to one another. Figure 8 illustrates one data frame which consists of one azimuth slit and the two 45 degree elevation slits. With this configuration the drum will pass the light source image through the slits three times for each data frame and the photomultiplier will

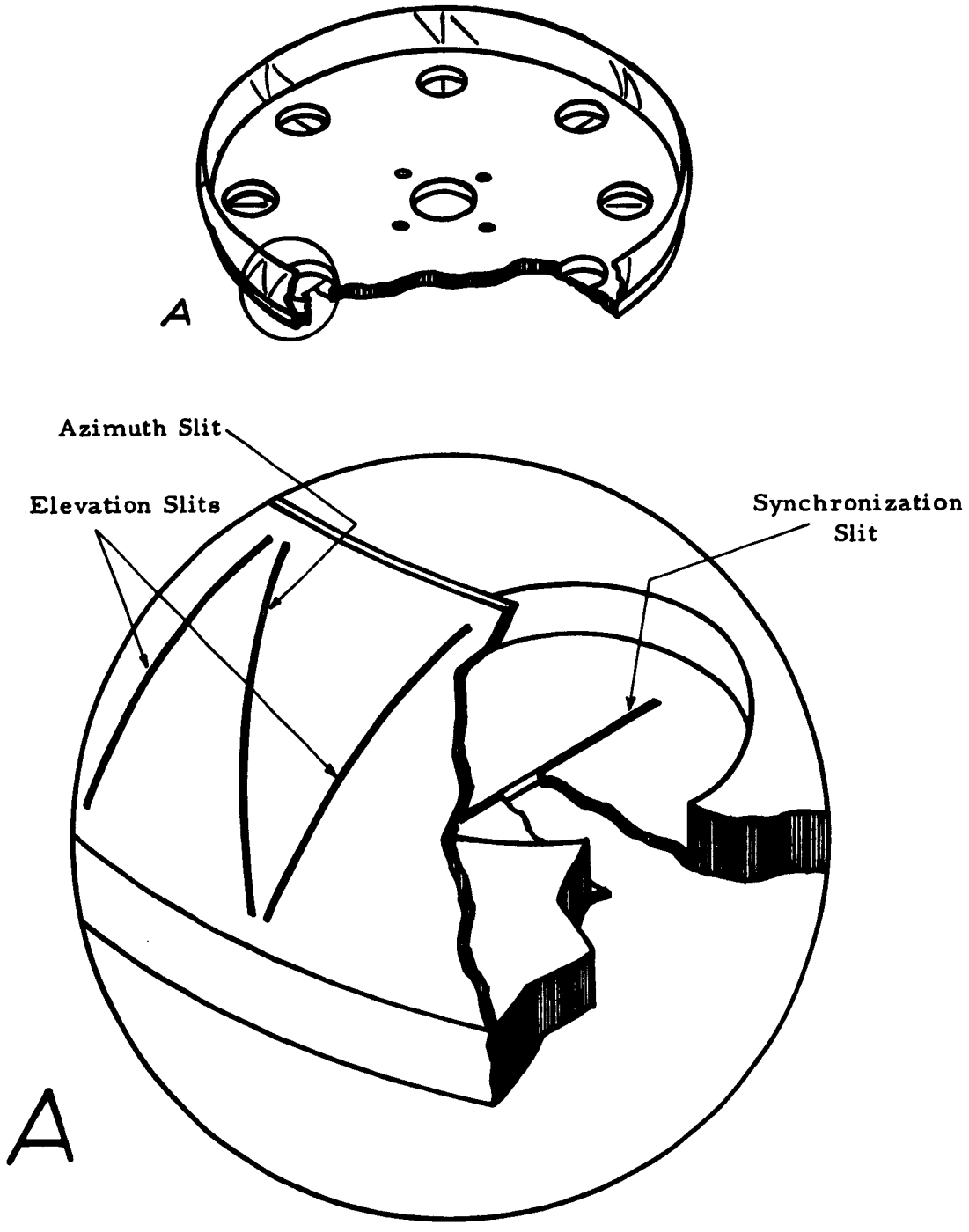

Isometric View of the
Rotating Spherical Section

Figure 8

produce three pulses per data frame. Of these three pulses, the center pulse continues to be the azimuth pulse because its occurrence relative to a time standard (sync pulse for example) will remain constant independent of any motion totally confined in an elevation plane. Any motion of the light source which has a component at right angles to the azimuth slit will provide a time displacement of the center pulse and this displacement will be proportional to azimuth.

For movement of the light source in an elevation plane, there will be movement of the image up or down on the drum. This movement will cause the time between pulse one and pulse two to change. Likewise the time between pulse two and pulse three will change. Figure 9 illustrates the time relationship of the pulses. The time duration from pulse one to pulse three is for all data frames a constant dependent upon the angular rate of the drum drive motor. The illustration in Figure 9 is based on an 1800-rpm motor. The ratio of the time interval separating pulse one and two, to the time interval separating pulse one and three is directly proportional to the elevation angle. The elevation angle (see the drawing) can be expressed as

$$E \sim \frac{a}{a + b}$$

When the ratio above is 1/2, the system is properly adjusted and the relative elevation angle is zero.

Additional details about the elevation slits, including a mathematical treatment of the geometry involved, are presented in the following chapter.

Figure 10 is an actual photograph of the oscilloscope showing the three target pulses in the upper photograph and one of the elevation pulses on an expanded sweep in the lower photograph. The dotted presentation is due to the multiplexing of the dual beam scope. The sweep time in the lower photograph is approximately 140 microseconds per inch. The image was not well focused for this picture and this caused the pulse length to be longer than usual.

The Synchronization System. - During consideration of the techniques for obtaining elevation coordinates with the 45° slits added to the drum, it became evident that a synchronization system was desirable. Coordinates are measured as functions of time; that is, the time relationship of the three data frame pulses describes the light source coordinates and provides an initial reference time pulse that is produced for a time reference. Figure 9 illustrates the time relationship of the data frame pulses to the sync pulse.

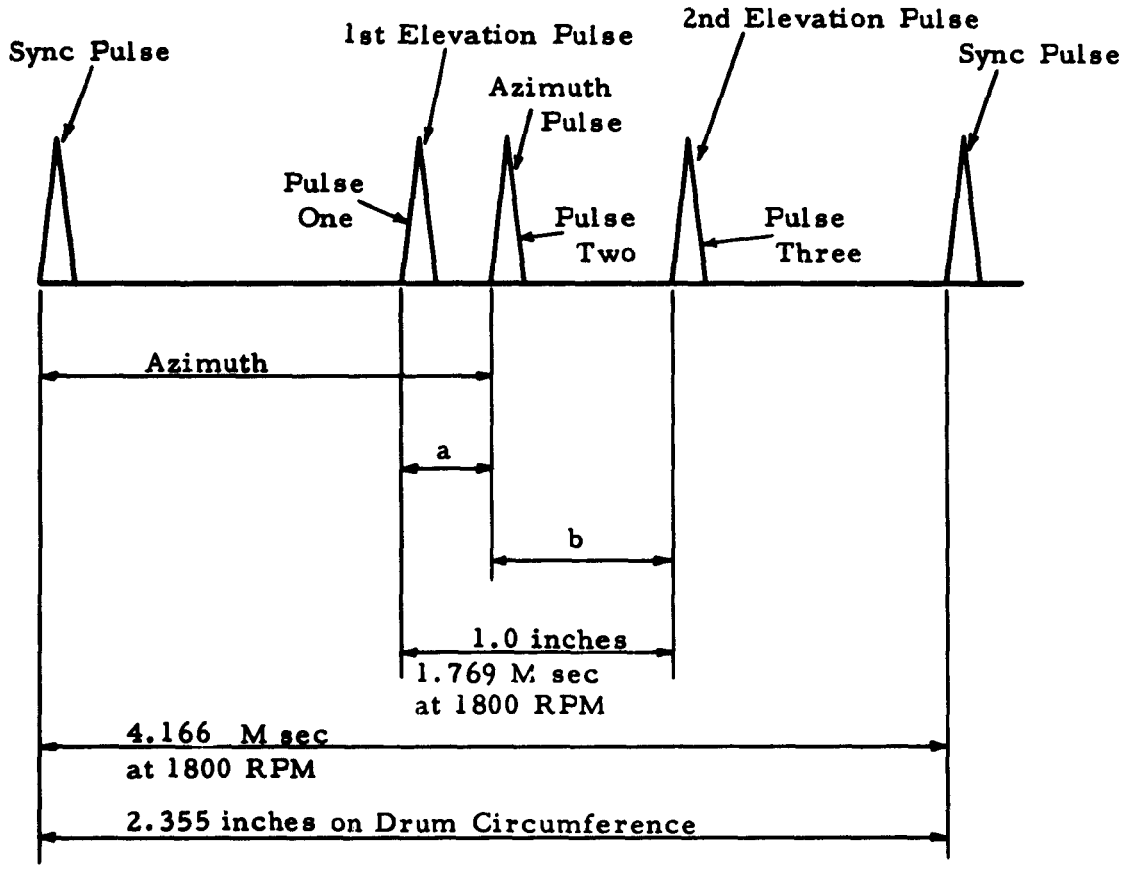

TIME RELATIONSHIP OF
OUTPUT PULSES

Figure 9

ONE DATA FRAME

Sync pulse is not included here

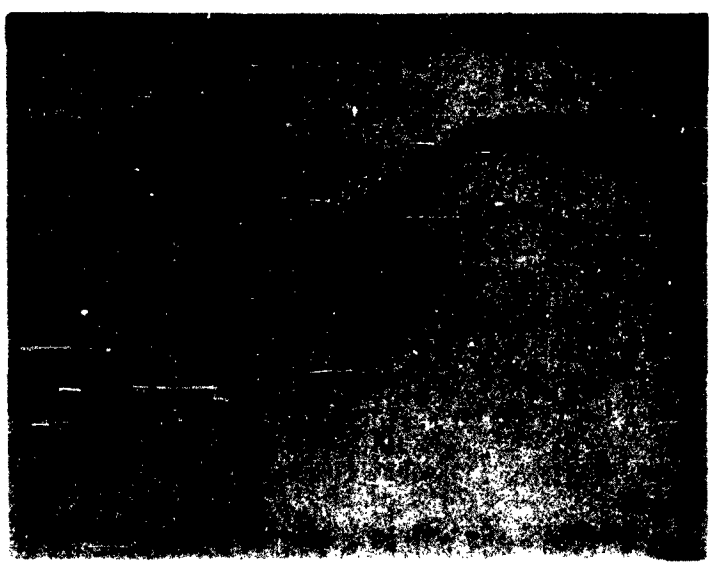

EXPANDED VIEW OF ELEVATION PULSE

(Note that camera shutter was open 4 data frames)

Figure 10

The synchronization pulses were added to the system by cutting eight slits in the base of the drum. These slits were centered timewise between the azimuth slits. A six-volt lamp, two short focal length lenses, and a pin hole were used to provide a continuous small spot of light in the region of the sync slits. An additional photo-multiplier was used to detect the light through the sync slits when the slits were coincident with the light spot. This technique proved to be very simple and reliable. A very stable reference is provided in this manner. A simple photosensitive detector rather than the photo-multiplier could have been used, but using off-the-shelf items led to this configuration.

IV. MATHEMATICAL ANALYSIS OF THE PERSEAS

Introduction. - The foregoing sections have given the general and detailed description of the PERSEAS. A simplified model may be adequate for a mathematical analysis. A function of the device is to pass light rays from a point source on a target, through a lens of constant orientation, and thence to a focus on the periphery of a rotating drum. The drum has slits cut in the periphery, and as these slits pass the focused light spot, the light goes through to cause a photomultiplier tube to operate and generate a time signal. These time signals are the data to be used to find the angular coordinates of the light source relative to the PERSEAS. In this analysis the drum is supposed to have a spin axis of constant orientation and have a constant spin velocity. However, it will be seen that the relative angular coordinates are found to be free of assumptions of the actual spin rate, so that some variations from a constant spin rate may be of small consequence to the accuracy of the results.

It may be seen that one action of the lens is to generate a transformation of points, from object space to image space. The image space is the focal surface of the lens while the object space is three-dimensional. While each object point has a unique image point, the converse is not true. The relation between object points and image points may best be determined by test, or calibration. However, theory may be of use in such calibration. It has been shown that for the purposes of an analysis of the geometrical relations between object points and image points of a lens, the lens may sometimes be replaced by a mathematical model of a projection center, Reference 1. This projection center is merely a fixed point through which light rays from any object point pass on a straight line path to the corresponding image point. With an origin of relative coordinates located at such a projection center, there is then a one-to-one correspondence between image points and the relative angular coordinates of points in object space. In other words, all points in object space along the same ray from this origin have a common image point. If the origin were located in such a favored position, the calibration could be made to be independent of range, and dependent only on the angular coordinates.

Also, for such an ideal lens with the proper orientation of axes, there are linear relations between the angular coordinates in object space and the angular coordinates in image space.

It has been stated that the problem of relating the points in object space to those in image space is best solved by calibration, with some theory as a guide. The problem of relating the coordinates of points in image space to the data (times of light spot crossing of slits) will be investigated in this section. These relations are intermediate to those relating the points in object space to the data.

Substitutions could then be made to give the desired correspondence between the relative angular coordinates of points in object space and the data. Such correspondences could always be set up through experimentation, but theoretical relations may provide useful information, and may be more satisfactory than purely empirical relations for purposes of analysis, curve fitting, least squares adjustment of data, etc.

It should be kept in mind that in the following discussion relations are to be determined for the coordinates of the focused light spot in terms of the data. These coordinates of the light spot are not those of the light source, nor are the time derivatives the same; however, there is good reason to believe that the correspondences between the selected angular coordinates of the light spot and those of the light source are approximately linear. The nature of the correspondences between object points and the data may thus be inferred from the relations between image points and the data.

The material in this section entitled "Analysis of a Simplified Model" has appeared previously in the Contract Monthly Notes. It is included here for completeness.

Analysis of A Simplified Model. - Light from a point source on a target passes through a lens of constant orientation and is brought to a focus at the periphery of a rotating cylindrical section, which will be referred to hereafter as a drum. The drum has slits cut in its periphery, and as a slit passes the focused light beam the light goes through the slit to be sensed by a photoamplifier tube, the output of which may be interpreted as a time signal. Various slit configurations have been considered which permit a known rotational rate, ω, of the drum, and the time signal data to be combined to give the azimuth and elevation angular coordinates of the light source.

In this present mathematical model, the drum is taken to be a section of a circular cylinder. This model is a simplification of the drum actually used at the Military Physics Research Laboratory for an experimental angle-sensing device, in which the drum is a section of a sphere. This simplified mathematical model considered here permits a more simple analysis of the geometrical relations required to interpret the data; in a sense, it forms a limiting case for the spherical drum as the drum section grows smaller. Actually the linear relations which may be derived for the relative angular coordinates for this cylindrical drum also apply over appreciable intervals for a spherical drum, and serve as a useful check on the relations which apply for the spherical drum. The geometrical relations for the spherical drum will be presented in the following section of this report.

Figure 11 is a sketch of the rotating drum, with the present slit configuration. A set of reference axes of fixed orientation is also shown, with the z-axis collinear with the spin axis of the rotating drum and with the origin at some convenient location along the spin axis. In the full scale scoring device, a number of identical slit groupings of this type would be located around the drum periphery. Also, the drum might be truncated, so that the slits do not intersect on the drum itself.

Consider the light spot to be somewhere on slit 1 at time t_1, somewhere on slit 2 at time t_2, and somewhere on slit 3 at time t_3. Slits numbered 1 and 3 make the same constant angles with the direction of the z axis, so they may be thought of loosely as being parallel. If the drum surface were flattened out to a plane these lines 1 and 3 would be parallel. The slit 2 is parallel to the z axis. The times t_1, t_2, t_3 are the data produced by the device.

When the rotational rate, ω, of the drum is known, and initial reference values of time and drum position are known, then the time t_2 is a direct measure of the azimuth, $A(t_2)$, of the light spot. The height, h(t), of the light spot is similarly a direct measure of the elevation angle of the light spot. The value of $h(t_2)$ may be obtained by combining the time data. The angular coordinates of the light spot may be related to those of the light source by calibration.

The variables affecting the problem are $\dot{h}$, $\dot{A}$, and h. If $\dot{A}$ (the azimuth rate of the light spot) is equal to ω, it is readily seen that once the light spot is on line 2, it stays there indefinitely, so that no determination of h is possible.

In order to determine the influence of azimuth rate, $\dot{A}$, on the results, let the initial position of the lighted spot be on line 1 at t_1, and consider the drum stopped from rotating. During the time interval $(t_3 - t_1)$ the spot will have moved in the direction of rotation of the drum through the angle $(t_3 - t_1)\dot{A}$. Now let the drum rotate through this angle to put the spot back on line 1. No further consideration of $\dot{A}$ effects need be made for the time interval $(t_3 - t_1)$.

Now let the effects of elevation rate, $\dot{h}$, be considered. The variable h will have increased by the amount $(t_3 - t_1)\dot{h}$ during the time interval $(t_3 - t_1)$. In order to put the spot back on line 1, the drum would have to reverse and be rotated through the angle $(t_3 - t_1)\dot{h}\,\phi/\ell$.

Then the drum must be rotated through the angle ϕ to put the light

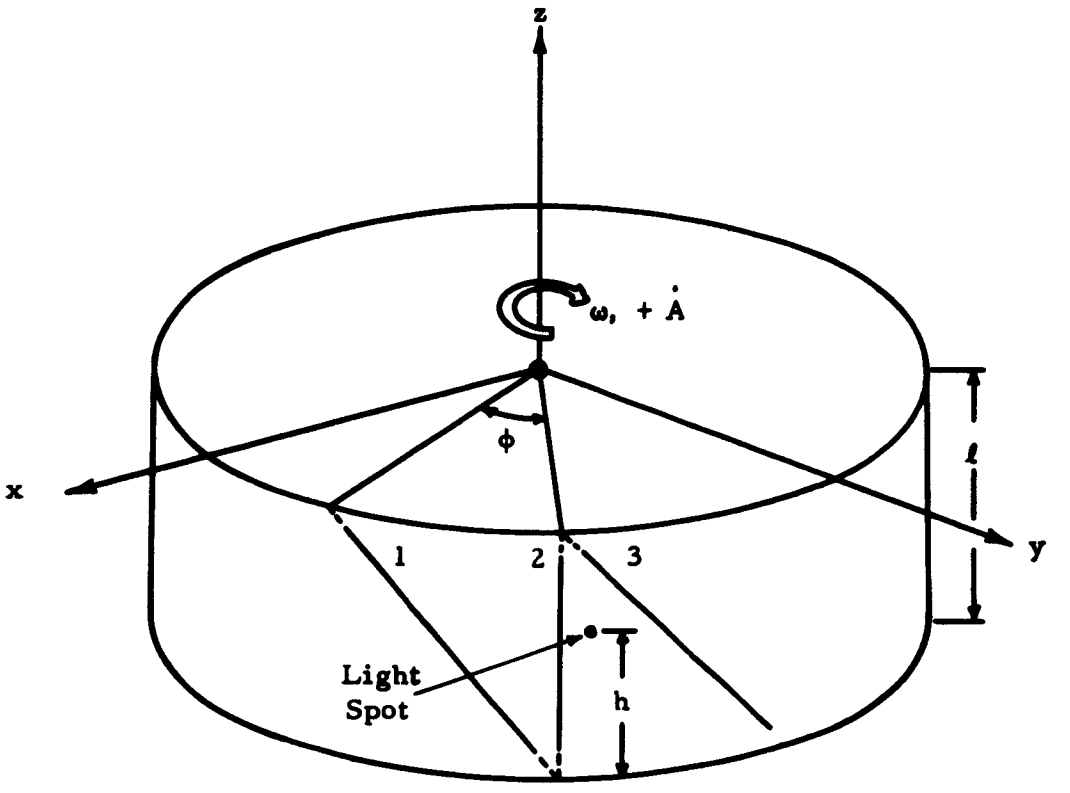

Figure 11

Slit Arrangement of the PERSEAS

spot on line 3. Adding these rotations,

$$(t_3 - t_1)\dot{A} - (t_3 - t_1)\dot{h}\frac{\phi}{\ell} + \phi = (t_3 - t_1)\omega \qquad (1)$$

Solving for $\dot{h}$,

$$\dot{h} = \ell\left[\frac{\phi + (\dot{A} - \omega)(t_3 - t_1)}{(t_3 - t_1)\phi}\right] \qquad (2)$$

If $|\dot{A}| << |\omega|$, equation 2 may be used to get an approximate value of $\dot{h}$. However, so long as $\dot{A}$ and ω may be considered constant during the time interval $(t_3 - t_1)$, one may still find $h(t_2)$. Let $h_1 = h(t_1)$, $h_2 = h(t_2)$, and $h_3 = h(t_3)$. Then $h_1 = h_2 - \dot{h}(t_2 - t_1)$.

Adding the drum rotations during the time interval $(t_2 - t_1)$ in a similar manner as previously, but taking these component rotations in the order $\dot{A}$, ϕ, and h, one gets

$$(t_2 - t_1)\dot{A} + \frac{\phi}{\ell} h_1 = \omega(t_2 - t_1) \qquad (3)$$

Solving for h_1,

$$h_1 = \frac{\ell}{\phi}(t_2 - t_1)[\omega - \dot{A}]$$

Then

$$h_2 = h_1 + (t_2 - t_1)\dot{h}$$

and substituting the value for $\dot{h}$ from equation (2)

$$h_2 = \left[\frac{t_2 - t_1}{t_3 - t_1}\right]\ell \qquad (4)$$

Equation (4) holds for any constant $\dot{h}$, $\dot{A}$, and is independent of them. To avoid small divisors, the time interval $(t_3 - t_1)$ should be reasonably large, so that ϕ should be fairly large from this viewpoint. Similarly, truncating the drum and/or making a fairly large angle between slits 1 and 2 should help to make the determination of h_2 more precise. Other (engineering) considerations would have to be taken into account in decisions on these points.

It might be thought that the time interval $(t_3 - t_2)$ might contribute

new information. The equation for the rotations during the time interval $(t_3 - t_2)$ is

$$\phi - \frac{h_3\phi}{\ell} + \dot{A}\,(t_3 - t_2) = \omega(t_3 - t_2) \tag{5}$$

$$h_3 = \ell + \frac{\ell}{\phi}\,(t_3 - t_2)[\dot{A} - \omega]$$

$$h_2 = h_3 - \dot{h}(t_3 - t_2)$$

$$h_2 = \frac{t_2 - t_1}{t_3 - t_1}\,\ell\,, \text{ which is the same result as equation 4.}$$

In fact, equation (1) is just the sum of equations (3) and (5). These three basic equations then have a determinant of zero, so that all possible information has been extracted from them.

An alternate slit configuration is shown in Figure 12. Slits one and three of this configuration are parallel to the z axis. An analysis similar to the preceding ones for the drum rotations shows that

$$h(t_2) = \frac{t_2 - t_1}{t_3 - t_1}\,\ell \tag{6}$$

In addition, one gets $A(t_1)$, $A(t_2)$, $A(t_3)$, and $\dot{A}$, and also, some space on the drum may be conserved.

Another alternate slit grouping is similar to the one first considered, except that two extra slits have been added, these being lines parallel to the z axis at each end of the group, see Figure 13. These take up no additional space on the drum, and yield considerable extra information. With this slit arrangement, one may compute $A(t_2)$, $h(t_2)$; $A(t_3)$, $h(t_3)$; $A(t_4)$, $h(t_4)$; also $A(t_1)$, $A(t_5)$, and $\dot{A}$ and $\dot{h}$. The values of $h(t_2)$, $h(t_3)$ and $h(t_4)$ may be computed from more than one set of data; there is redundancy in the data, therefore. Least squares data adjustment could be used if considered appropriate. Other refinements possible are those which permit $\dot{A}$ and $\dot{h}$ to have different (constant) values over different time intervals, with use being made of the equations derived in this note.

These equations could also be differentiated to give the linear relations for the errors, and averaged statistically to give variance relations.

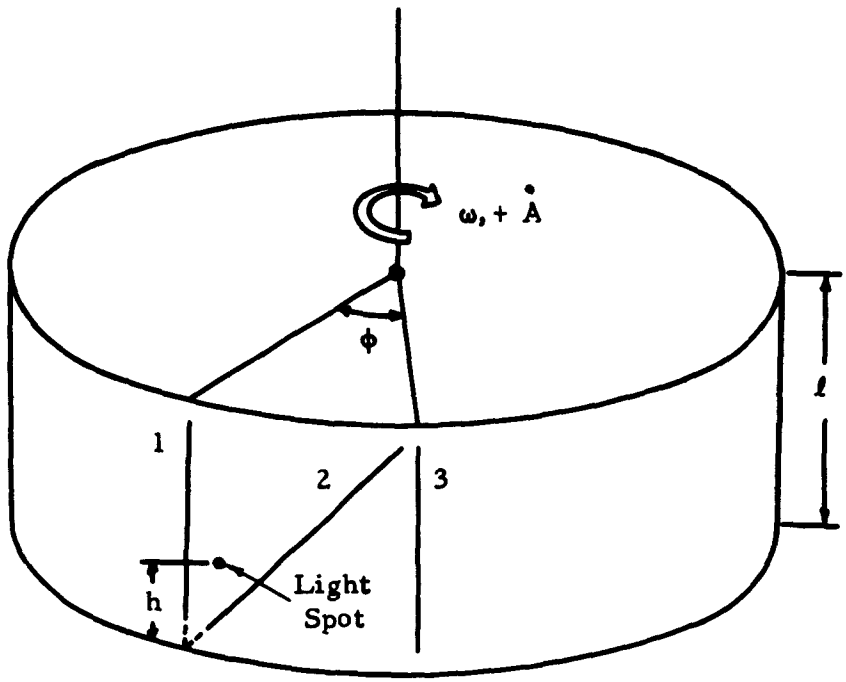

Figure 12
Alternate Slit Arrangement of the PERSEAS

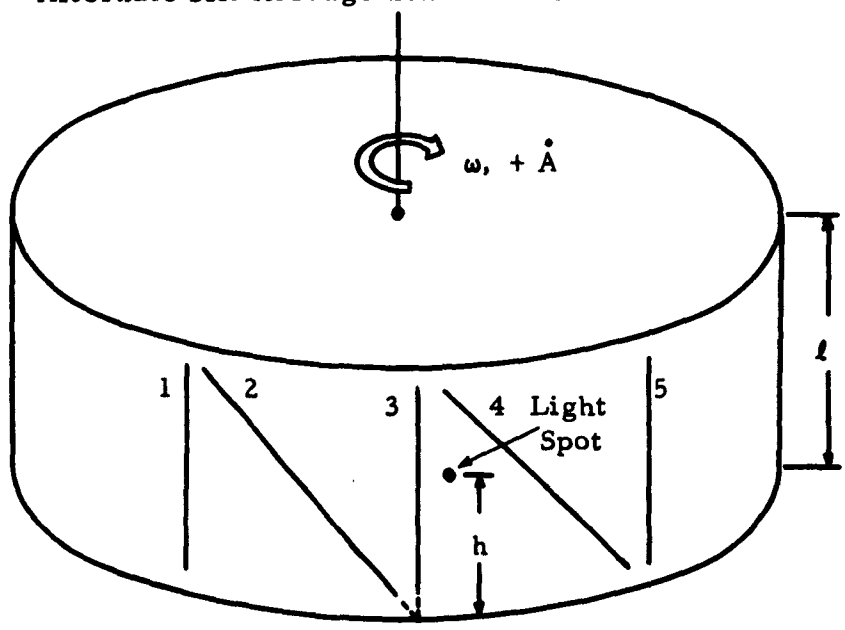

Figure 13
Another Slit Arrangement Which will Produce Redundancy in the Data

Analysis of the PERSEAS. - An experimental model of the PERSEAS differs from the model described in the previous section in that the circular cylindrical drum of the previous model is replaced with a drum which is a section of a sphere, see Figure 14. The slits are great circles on the sphere. The figure shows a group of slits where, for clarity, the scale has been distorted. Slits numbered one and three are inclined at an angle β to the equator of the drum, while slit number two is vertical and makes a 90^{o} angle with the equator of the drum. The actual drum has a number of such slit groupings equally spaced about the drum periphery.

The azimuth coordinates of the focused light spot relative to some reference direction will be considered briefly. The basic azimuth coordinate scheme has been discussed previously; the time at which the light spot crosses a vertical slit is a direct measure of the azimuth of the light spot. Also, an azimuthal direction of fixed orientation for reference is established and as a vertical slit of the rotating drum crosses this reference direction a time signal is generated. The time interval between such reference timing pulses is a measure of the angular velocity, ω, of the rotating drum. Thus a constant check on the current values of ω is available. If $\omega(t)$ were required, it would be given sufficiently accurately by a relation of the form $\omega(t) = 2\pi/[t_n - t_{n-1}]$, where $[t_n - t_{n-1}]$ is the time interval between the most recent successive crossings of the reference azimuthal direction by the same vertical slit. Similarly, with t_k the time at which any particular vertical slit passed the reference direction and t the next later time at which the focused light spot also crosses this particular slit, then the azimuth angle, A(t), of the light spot relative to the reference direction is given for this time, t, by

$$A(t) = \omega [t - t_k] = 2\pi \left[\frac{t - t_k}{t_k - t_{k-1}} \right]$$

The azimuth of the light spot relative to any other desired constant direction in the plane of the equator of the spherical drum and passing through the center of this sphere is then given by this last expression plus a constant. One should note that the azimuth coordinates of the focused light spot are independent of any assumptions about the actual value of ω, but may be expressed exclusively in terms of the time data. Thus, some variation in ω during scoring applications may be unimportant to the accuracy of the coordinate determinations. Also, the method actually used to periodically determine the orientation of the drum relative to a fixed azimuthal direction may be different from the one described here without affecting the form of the relation between the azimuth coordinates of the focused light spot and the time signals generated by the light spot crossing a vertical slit.

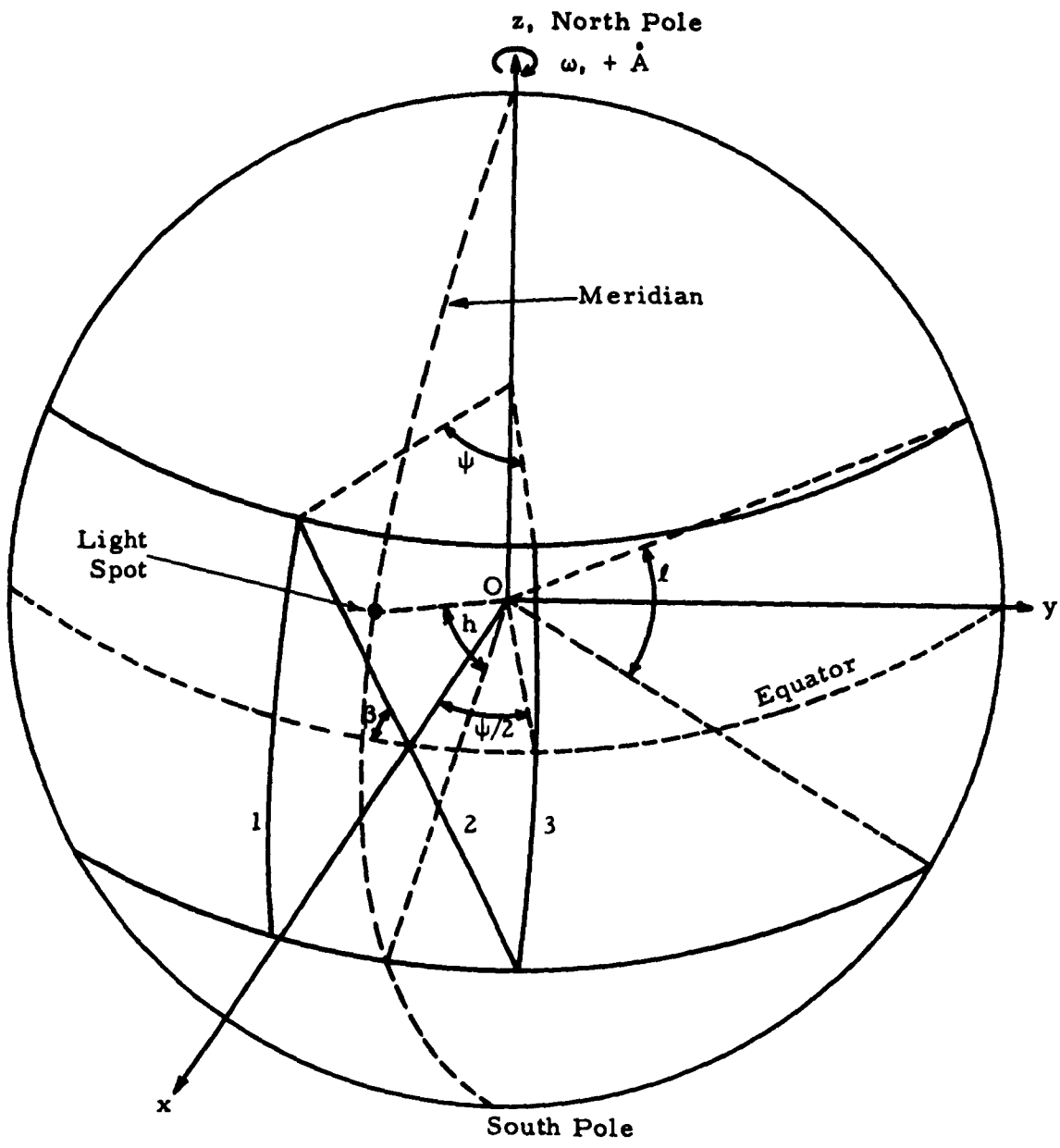

Figure 14

Alternate Slit Arrangement

The elevation coordinate, h(t), at which the light spot crosses a slit (whether vertical or slanting) may also be found. It will be convenient to use h as the angle measured at the center of the spherical drum. Then h is the difference in latitudes of the light spot and the latitude parallel passing through the lower intersection of the slanted and vertical slits, see Figure 14.

The assumptions will be made that the time derivatives of the angular coordinates of the focused light spot, $\dot{h}$ and $\dot{A}$, as well as ω, are constant during the time interval required for the light spot to cross slits one, two, and three of Figure 14. It will also be assumed that during this time interval h is a linear function of t, $h(t) = h(t_o) + (t - t_o)\dot{h}$, with t and t_o any times on the interval (t_1, t_3); and that a certain function of h to be described later is given by its linear terms of a Taylor's series on this interval. The light spot is on line one at $t = t_1$, with $h(t_1) = h_1$; similarly, $h(t_2) = h_2$ and $h(t_3) = h_3$.

In Figure 14 a set of non-rotating coordinate axes is shown with origin, O, at the center of the sphere, z axis aligned with the spin axis, and x axis in the plane of the equator of the drum, passing through slit number one. This orientation is chosen as an aid to determining the relation between h and longitude along slit number one. If one considers the sphere of the drum to be of unit radius, the equations of the great circle forming slit number one and intersecting the x axis are given by

$$\begin{aligned} x^2 + y^2 + z^2 &= 1 \\ z \cos\beta + y \sin\beta &= 0 \end{aligned} \qquad (1)$$

Since the spherical drum rotates about a constant axis, it will also be convenient to have an auxiliary system of latitude and longitude coordinates as indicated. Latitude is measured north and south of the equator and longitude is measured from east to west, with the longitude of the x axis taken to be zero. The longitude difference of two points is thus the drum rotation which separates them. The conversion from h to latitude is obvious,

$$\begin{aligned} &\text{Lat (N of Equator)} = h - \frac{\ell}{2} \\ &z \text{ (on great circle No. 1)} = \sin \text{Lat} = \sin\left(h - \frac{\ell}{2}\right) \end{aligned} \qquad (2)$$

Here, the quantities h and ℓ are measured in radians. The longitude of any point x, y, z located on great circle number one is given by:

$$\sin \text{long} = -y / \sqrt{x^2 + y^2} \qquad (3)$$

It may be shown that the longitude separation of any two points at the same latitudes on slits one and three is a constant, ψ. When substitutions are made from equations (1) and (2), into equation (3), there results

$$\sin \text{long} = \tan \left(h - \frac{\ell}{2}\right) \cot \beta \tag{4}$$

This equation (4) will be useful in finding equations for the drum rotations due to changes in the h coordinate of the light spot.

If one proceeds to add the drum rotations required over the time interval (t_1, t_2) in the same manner as that used in the preceding section, one sees that the effect of $\dot{A}$ over this time interval is to require a rotation of amount $(t_2 - t_1)\dot{A}$, which leaves the lighted spot on line one at h_1. If the drum is then rotated to put the spot on slit two, use of equation (4) shows that the additional rotation necessary is

$$\frac{\psi}{2} + \sin^{-1}\left[\tan\left(h_1 - \frac{\ell}{2}\right) \cot \beta\right] \tag{5}$$

The further change from h_1 to h_2 requires no additional rotation of the drum. Adding these rotations gives

$$(t_2 - t_1)\dot{A} + \frac{\psi}{2} + \sin^{-1}\left[\tan\left(h_1 - \frac{\ell}{2}\right)\cot \beta\right] = (t_2 - t_1)\omega \tag{6}$$

Similarly, for the time interval (t_2, t_3) there results

$$(t_3 - t_2)\dot{A} + \frac{\psi}{2} - \sin^{-1}\left[\tan\left(h_3 - \frac{\ell}{2}\right) \cot \beta\right] = (t_3 - t_2)\omega \tag{7}$$

A third equation, for the drum rotation over the entire time interval, (t_1, t_3), is just the sum of these last two equations:

$$(t_3 - t_1)A + \psi + \left\{\sin^{-1}\left[\tan\left(h_1 - \frac{\ell}{2}\right) \cot \beta\right] - \sin^{-1}\left[\tan\left(h_3 - \frac{\ell}{2}\right) \cot \beta\right]\right\} = (t_3 - t_1)\omega \tag{8}$$

If the two quantities within the braces of this last equation are replaced by the linear terms in their Taylor's series expansions about the point h_2, there results

$$\psi - \dot{h}(t_3 - t_1) \frac{\sec^2(h_2 - \frac{\ell}{2}) \cot\beta}{\sqrt{1 - \tan^2(h_2 - \frac{\ell}{2}) \cot^2\beta}} = (t_3 - t_1)(\omega - \dot{A}) \tag{9}$$

or

$$\frac{\dot{h} \sec^2(h_2 - \frac{\ell}{2}) \cot\beta}{\sqrt{1 - \tan^2(h_2 - \frac{\ell}{2}) \cot^2\beta}} + (\omega - \dot{A}) = \psi/(t_3 - t_1) \tag{10}$$

If the arc sine in equation (6) is similarly expanded about the point h_2 there results:

$$\frac{\psi}{2} + \sin^{-1}\left[\tan(h_2 - \frac{\ell}{2}) \cot\beta\right] - \frac{\dot{h}(t_2 - t_1)\sec^2(h_2 - \frac{\ell}{2})\cot\beta}{\sqrt{1 - \tan^2(h_2 - \frac{\ell}{2})\cot^2\beta}} \tag{11}$$

$$- (t_2 - t_1)(\omega - \dot{A}) = 0$$

Substitution from equation (10) into this last equation to eliminate $\dot{h}$, $\dot{A}$, and ω gives

$$\sin^{-1}\left[\tan(h_2 - \frac{\ell}{2}) \cot\beta\right] = -\frac{\psi}{2} + \frac{t_2 - t_1}{t_3 - t_1}\psi \tag{12}$$

or

$$\tan(h_2 - \frac{\ell}{2}) \cot\beta = \sin\psi\left[\frac{2(t_2 - t_1) - (t_3 - t_1)}{2(t_3 - t_1)}\right] \tag{13}$$

In this equation there is the single unknown h_2, so its value may be found. Once the value of h_2 has been found, it could be used in equation (10) to further define this constraint on the values of $\dot{h}$, $\dot{A}$, and ω. This constraint, and the value of h_2, as well as $A(t_2)$, are all the information that may be obtained from the data assumed. The expansion of the arc sine of equation (7) in a similar fashion to that

used with equation (6) leads to equation (13) as before. As the determinant of the linear versions of the three basic equations (6), (7), and (8), has a value of zero, no additional unknowns may be evaluated from this data.

Equation (13) may be solved for the value of h_2 to any required degree of approximation by the use of Taylor's series with only linear terms retained. In such procedures, an approximate value of h_2 is assumed, and a correction is found. Iteration may then be used to improve the precision to the extent desired. The convergence is much faster when the first assumed value of h_2 to satisfy equation (13) is close to the correct value. Fortunately, a good first estimate of h_2 is provided by the analysis of the last section,

$$h_{2,0} = \ell \frac{t_2 - t_1}{t_3 - t_1} \tag{14}$$

Thus,

$$h_{2,1} = \ell \frac{t_2 - t_1}{t_3 - t_1} - \frac{\tan \ell \left[\frac{2(t_2 - t_1) - (t_3 - t_1)}{2(t_3 - t_1)}\right] \cot \beta - \sin \psi \left[\frac{2(t_2 - t_1) - (t_3 - t_1)}{2(t_3 - t_1)}\right]}{\sec^2 \ell \left[\frac{2(t_2 - t_1) - (t_3 - t_1)}{2(t_3 - t_1)}\right] \cot \beta}$$

. . .

$$h_{2,n} = h_{2,n-1} - \frac{\tan (h_{2,n-1} - \frac{\ell}{2}) \cot \beta - \sin \psi \left[\frac{2(t_2 - t_1) - (t_3 - t_1)}{2(t_3 - t_1)}\right]}{\sec^2 (h_{2,n-1} - \frac{\ell}{2}) \cot \beta}$$

One may note that equation (4) may be used to obtain the relation

$$\tan \frac{\ell}{2} \cot \beta = \sin \frac{\psi}{2} \tag{16}$$

These relations indicate that the initial approximation $h_{2,0}$ should have no error when $h_2 = 0$, $\ell/2$, or ℓ.

The first approximation, equation (14), to the value of h_2 required to satisfy equation (13) is seen to have no error at $h_2 = 0$, $\ell/2$, and ℓ. For the present device (ℓ, ψ, and β specified), a numerical check shows the maximum error of the first approximation, $h_{2,0}$, is only a fraction of a milliradian, with the error an odd function of $\left[\frac{t_2 - t_1}{t_3 - t_1} - \frac{1}{2}\right]$ which could be fitted quite accurately with either a simple sine or algebraic correction term. Also, a single iteration, equation (15), would provide all the accuracy needed to solve equation (13). For linear relations between the elevation coordinate, E, of the light source, and the coordinate, h, of the light spot, one then theoretically has linear relations between $E(t_2)$ and $(t_2 - t_1)/(t_3 - t_1)$, except for a correction term with a maximum absolute value less than a milliradian.

An alternate slit arrangement is shown in Figure 15. Again, the slits are great circles on the spherical drum. Slits numbered one and three in this figure are vertical slits, or longitude meridians, while slit number two is inclined at the angle β to the equator of the drum. Again the assumptions will be made that $\dot{h}$, $\dot{A}$, and ω are constant over the time interval (t_1, t_3). From an initial condition with the light spot on slit number one at t_1, first let h_1 increase to h_2. No rotation of the drum is required, the lighted spot remaining on slit number one. Then let A increase by the amount $(t_2 - t_1)\dot{A}$. This amount of rotation of the drum would be needed to keep the spot on slit number one at h_2. Then rotate the drum to put the light spot on slit number two at h_2. Equation (4) indicates that here a drum rotation is needed, amounting to

$$\frac{\psi}{2} - \sin^{-1}\left[\tan\left(h_2 - \frac{\ell}{2}\right) \cot \beta\right] \tag{17}$$

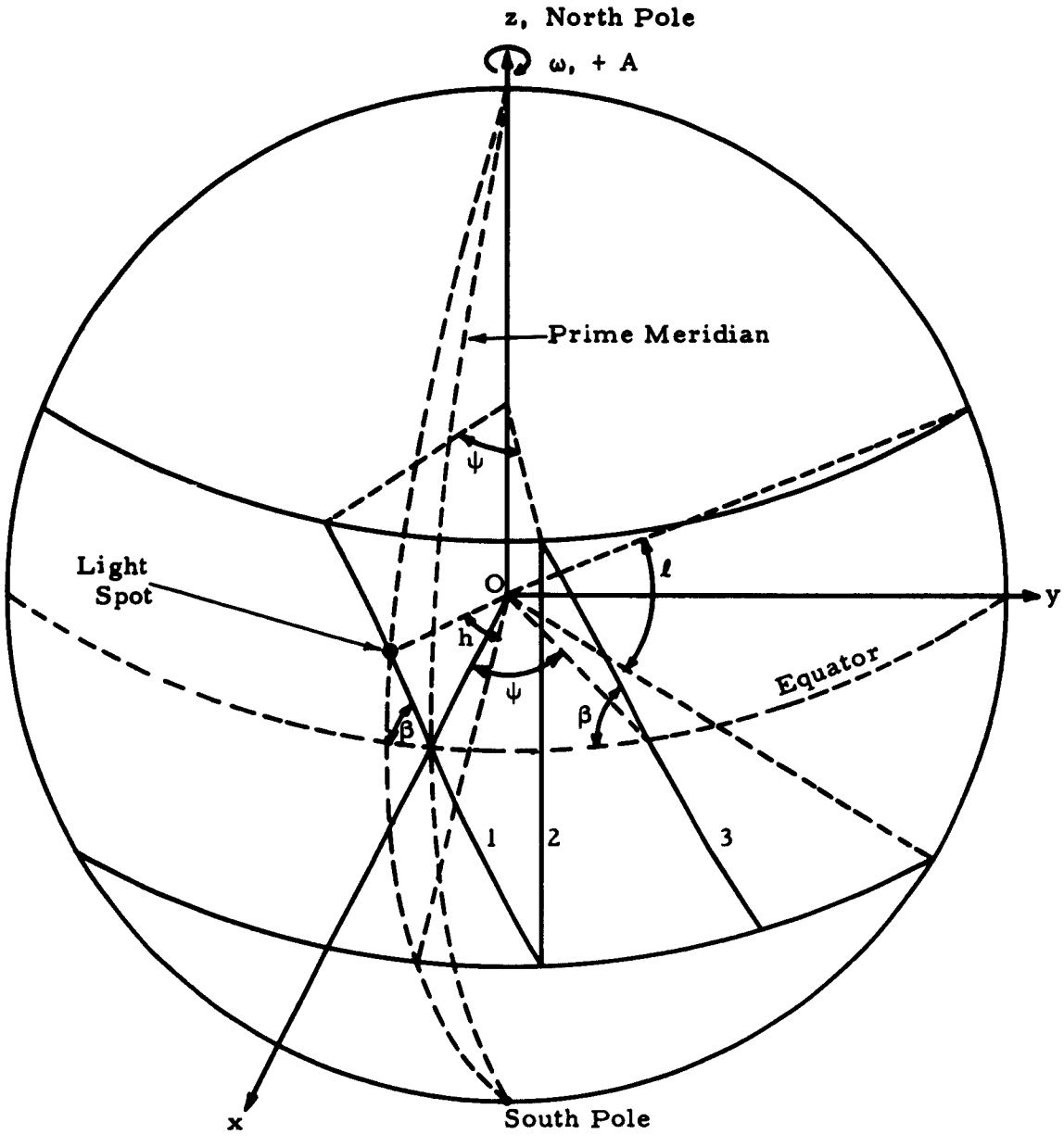

Figure 15

Spherical Drum with Slit Arrangement and Coordinate Systems

Adding these rotations,

$$(t_2 - t_1)\dot{A} + \frac{\psi}{2} - \sin^{-1}\left[\tan\left(h_2 - \frac{\ell}{2}\right)\cot\beta\right] = (t_2 - t_1)\omega \qquad (18)$$

Similarly, for the rotation over the time interval (t_2, t_3) there results:

$$(t_3 - t_2)\dot{A} + \frac{\psi}{2} + \sin^{-1}\left[\tan\left(h_2 - \frac{\ell}{2}\right)\cot\beta\right] = (t_3 - t_2)\omega \qquad (19)$$

Adding these last two equations, there results

$$(t_3 - t_1)\,\dot{A} + \psi = (t_3 - t_1)\omega \qquad (20)$$

Whence,

$$(\omega - \dot{A}) = \psi/(t_3 - t_1)$$

Substituting for $(\omega - \dot{A})$ into equation (19) gives

$$\tan\left(h_2 - \frac{\ell}{2}\right)\cot\beta = \sin\psi\left[\frac{2(t_3 - t_2) - (t_3 - t_1)}{2(t_3 - t_1)}\right] \qquad (21)$$

In this equation there is a single unknown, h_2, so that its value may be found. This same equation results when the value of $(\omega - \dot{A})$ from equation (20) is substituted into equation (18). Equation (21) may be solved to any required degree of approximation by the same method used to solve equation (13), iterating here from an initial approximate value for $h_{2,0} = \ell\left[\frac{t_3 - t_2}{t_3 - t_1}\right]$.

The azimuth coordinate also needs to be found for $t = t_2$. The assumption having been made that the azimuth rate $\dot{A}$ is constant over the time interval (t_1, t_3), the azimuth of the light spot is a linear function of the time,

$$A(t_2) = A(t_1) + \frac{t_2 - t_1}{t_3 - t_1}\left[A(t_3) - A(t_1)\right] \qquad (22)$$

Related Problems for Further Investigation. - The preceding analysis is for a simple mathematical model, with assumed ideal operating characteristics. The actual device must be supposed to function only approximately according to that of the mathematical model. Whereas the light has been supposed to generate an "instantaneous" correspondence between object and image points and an "instantaneous" correspondence is further supposed set up between image points and the time data, neither of these assumptions is exactly correct. It may be shown that for the relative velocities and ranges of interest for scoring applications, there is negligible time lag to the first of these correspondences. Considerable experiment may be necessary to determine the significant parameters of the latter correspondence.

Other subjects for further investigation desirable from the point of view of analysis include the following:

1. Analysis of optical system
2. Calibration procedures
3. Least squares data adjustment procedures applicable to calibration, instrument adjustments, and data reduction
4. Error analysis

V. EXPERIMENTAL RESULTS OF THE PERSEAS

The experimental studies of the PERSEAS concept were directed toward obtaining the important information which will ultimately describe the capability of a system constructed around the concept. The important information is

1. Response time
2. Sensitivity
3. Angular Measurement Accuracy

Photomultipliers have very fast response time. The 1P21 which was used in a good many of the studies has a response in the order of 10^{-8} seconds. In the Laboratory it was not possible to approach the response limit of the 1P21. The maximum speed that the drum was run was about 4500 rpm and with 0.004" slits the time per slit width is calculated to be about 3 microseconds. At this speed there was no indication that the response limit of the photomultiplier had been reached. This drum speed is several times faster than is required for the scoring problem, including orbital velocities.

The published sensitivity of the 1P21 tube is 80,000 microamperes per microwatt (see Reference 2). With a detector this sensitive one would not expect to experience sensitivity problems. In all of the experimental studies, both in the Laboratory and outside, it was necessary to attenuate the incoming light signal to prevent saturation of the photomultiplier. The 1P21 is a total energy device and it responds to light from any direction; therefore, scattered light through the lens, prism, and slits causes a noise signal to be generated. It is necessary for the signal energy to exceed the noise energy for the signal to be detectable. Thus, the primary problem is that of signal-to-noise ratio rather than signal strength alone. This problem has been studied briefly by using narrow band interference filters (100 Angstroms wide) to pass only selected portions of the spectrum. Most of the angular accuracy data was obtained using a 4730 Angstrom filter.

Wavelength Study. - Selection of wavelengths to study the PERSEAS was controlled primarily by the spectral responses of the various photomultiplier tubes. The visible region of the spectrum is largely covered by S-4 response tubes and in this region studies were made with 931A and 1P21 photomultipliers. The 1P21 is essentially the same as the 931A except that it has about 2½ times the gain. Two interference filters, each 100 Angstroms wide, were used for studies in the visible region. They were centered about 4730 Angstroms and 5380 Angstroms. Both of these filters were used in artificial light surroundings in the Laboratory and out in the open for

daytime and night time conditions. The only appreciable difference that could be detected in the performance with the two filters could be related directly to the spectral response of the tube at the filter wavelength. Signal-to-noise ratio for the two filters was about the same. Both filters prevented saturation except when looking at the sun.

Some studies were made in the infrared region of the spectrum using an amperex photomultiplier tube type 150 CVP (see Reference 3). This tube has an S-1 response. An interference filter 100 Angstroms wide centered at 8280 Angstroms was used with the 150 CVP tube. With an artificial lamp in the Laboratory, a fairly good signal-to-noise ratio could be realized but not as good as the 931A tube. Studies out in the open using the 150 CVP on a bright day led to the conclusion that there was a most unfavorable signal-to-noise ratio. The 1000-watt Xenon lamp could not be detected beyond about 20 ft. It was concluded that the 150 CVP was nearly saturated with noise and that the tube would have to be operated in a cold environment to reduce the noise appreciably. No additional studies were made in the IR region; however, it has not been concluded that this region is unusable for a device of this type. It was decided that more information could be obtained about the concept by working in the visible portion of the spectrum.

It should be noted here that PERSEAS is not a wavelength sensitive device. It will work in the IR, visible or UV spectrum with appropriate optics and photomultiplier tube. The device does not sense amplitude, wavelength or phase, the only requirement being a favorable signal to noise ratio.

Azimuth Accuracies. - Azimuth accuracies were measured in the Laboratory using the 931A photomultiplier and the 4730 Angstrom filter. Three sets of azimuth accuracy data were obtained at different distances using a 100-watt zirconium lamp with a red filter (see Figure 25). This data was taken under static conditions; that is, the lamp was moved to a fixed angle relative to the PERSEAS and the drum was rotated by hand to pass the image through the slit. With the image and slit coincident, as measured by the photomultiplier output on the oscilloscope, the drum angle was measured. This data was obtained before the elevation slits were added. Comparison of the drum angle to the light source angle was a measure of the azimuth accuracy.

The instrumentation for the azimuth accuracy data is shown in Figure 16. For a particular set of data, d_1 was held constant and d_2 was varied. The relative angle θ_A was computed.

$$\theta_A = \tan^{-1} \frac{d_2}{d_1}$$

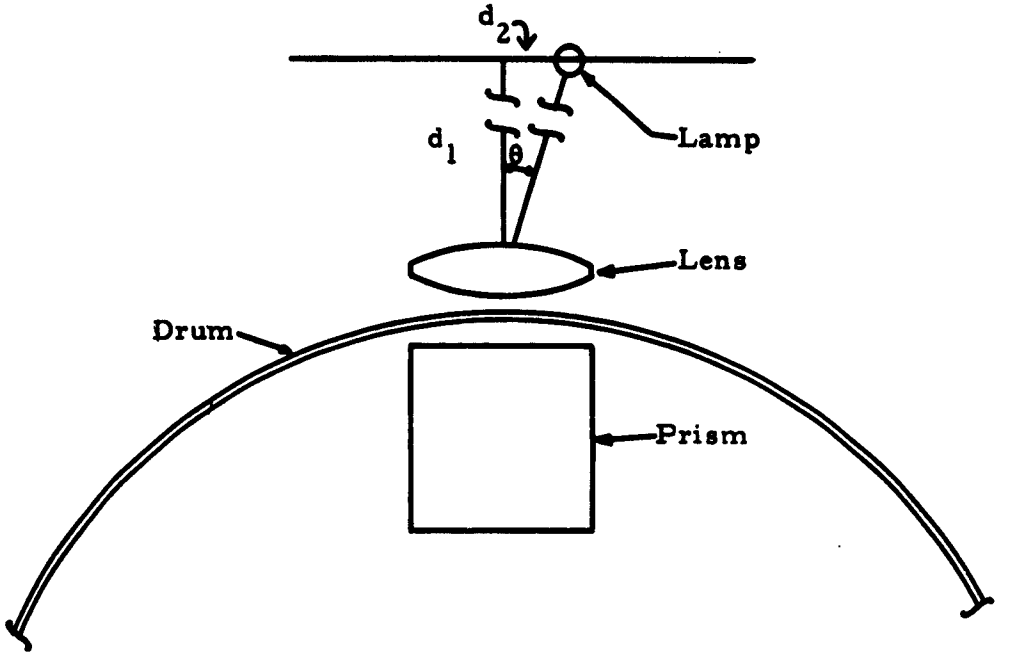

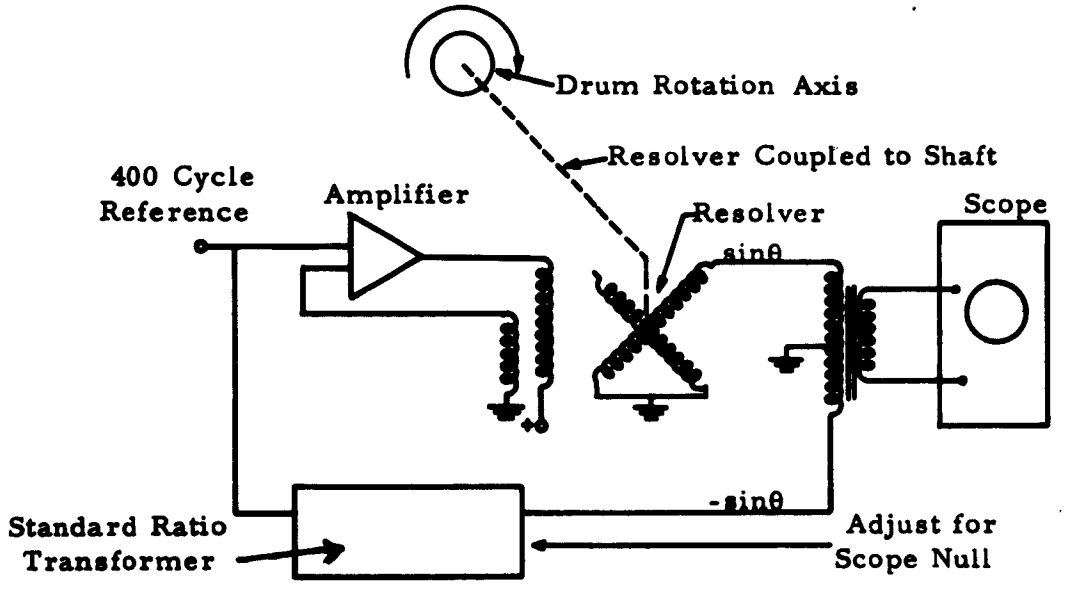

ELECTRONIC SETUP FOR STATIC
MEASURE OF AZIMUTH ACCURACY
OF PERSEAS

FIGURE 16

The drum angle, which is a direct measure of θ_A was measured by means of a resolver coupled directly to the drum axis. The output of the resolver sine winding (a 400 ~ signal) was compared with the output of a standard ratio transformer. The null signal resulting for the comparison was observed on an oscilloscope and when the null was minimized the standard ratio transformer was set to sin θ_A. A plot of the actual azimuth angle θ_A vs the resolver-measured angle shows that the system is linear within the resolution of the instrumentation used. The resolution limitation of the resolver is ± 1.5 milliradians. A plot of the azimuth data is shown in Figure 17.

After the elevation and synchronization slits were added to the drum, dynamic azimuth accuracy data was obtained by rotating the drum at 1800 rpm and measuring the time displacement of the azimuth pulse (see Figure 9) relative to the sync pulse. These measurements were made using a linear sweep oscilloscope and a stable sweep marker generator. Results of the dynamic azimuth data is shown in Figure 18. This data was taken over only 8 degrees of azimuth. It could have been taken at larger angles. Errors are within ± 1.5 milliradians. Repeated tests have shown that the present model is capable of consistently determining the azimuth angle of the target within this error range.

Elevation Accuracies. - Measurements of the PERSEAS elevation accuracies were made in the Laboratory using the 931A photomultiplier and the 4730 Angstrom interference filter. These measurements were repeated 3 times and in each set of data the entire slit system was operational; that is, all azimuth and elevation slits were open and the synchronizing pulses were used for the time reference. The drum speed was 1800 rpm; obtained from direct coupling to a synchronous motor. The electronic setup of measuring elevation accuracies is shown in Figure 19. The sync photomultiplier was used to trigger the gate generator and the oscilloscope sweeps A and B. The B scope trace was not used for accuracy measurements. Output from the azimuth and elevation slits were presented on the A trace for a fixed elevation angle.

Recalling that the three output pulses per data frame are found from the 2 elevation slits and the azimuth slit between them, it was necessary to measure time displacement from the first elevation pulse P_1 to the azimuth pulse P_2 and from P_2 to the second elevation pulse P_3 for each elevation angle. The time measurements were made by using the variable gate marker generator which was also synchronized with the sync photomultiplier. Accurate measurements of time from P_1 to P_2 and P_2 to P_3 required that the scope sweep be amplified

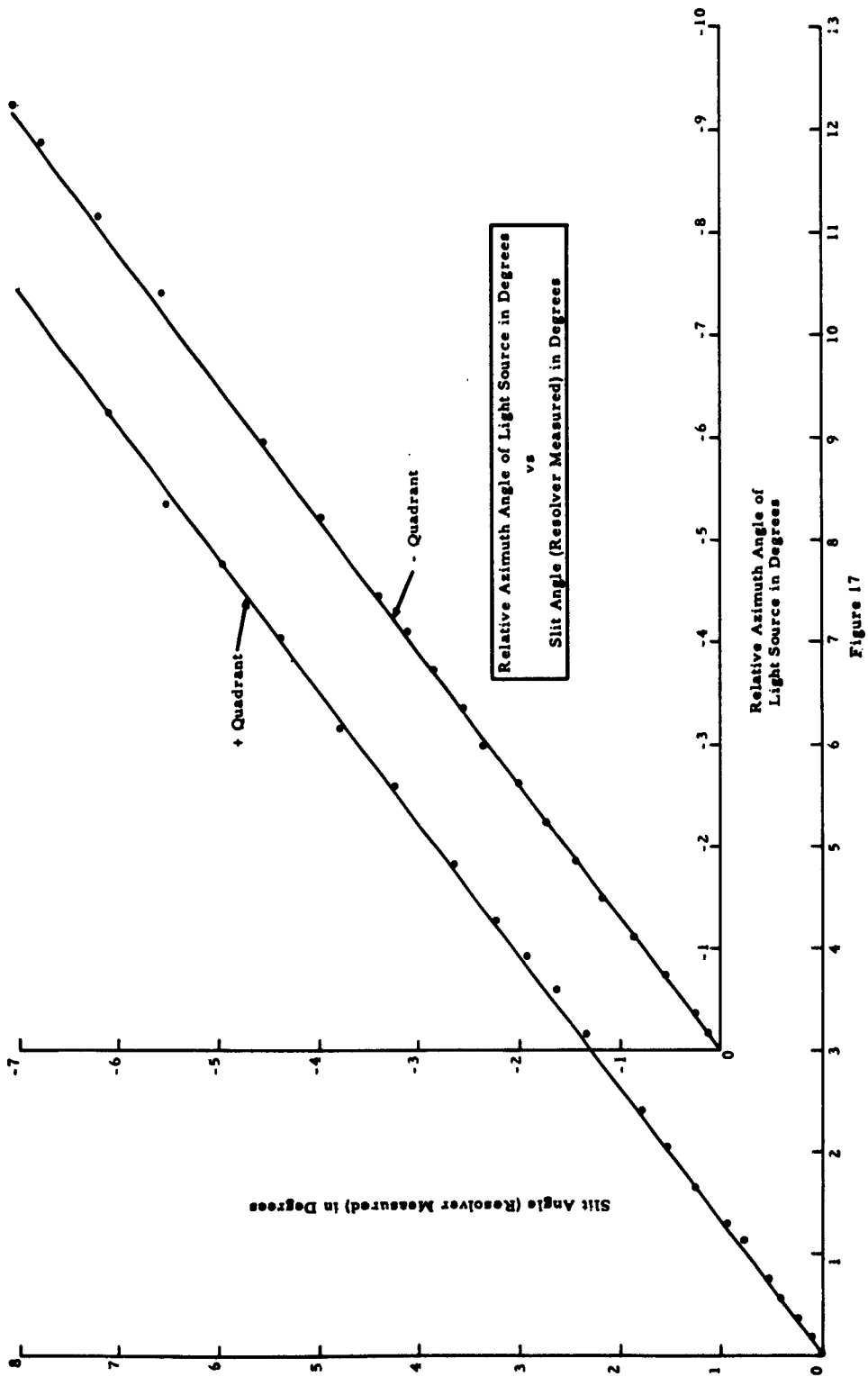
Relative Azimuth Angle of Light Source in Degrees
vs
Slit Angle (Resolver Measured) in Degrees
+ Quadrant
- Quadrant
Slit Angle (Resolver Measured) in Degrees
Relative Azimuth Angle of
Light Source in Degrees

Figure 17

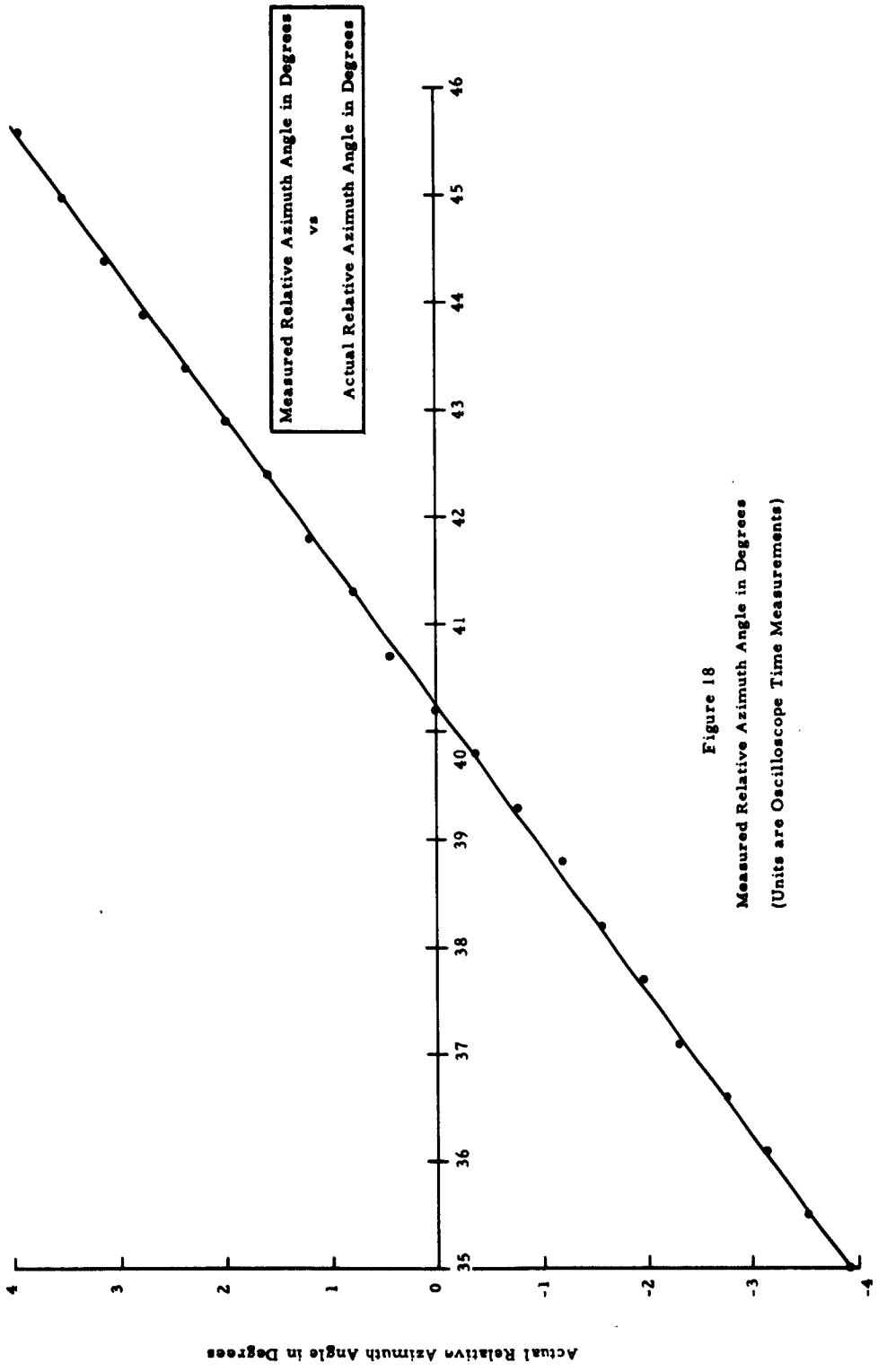

Figure 18

Measured Relative Azimuth Angle in Degrees

(Units are Oscilloscope Time Measurements)

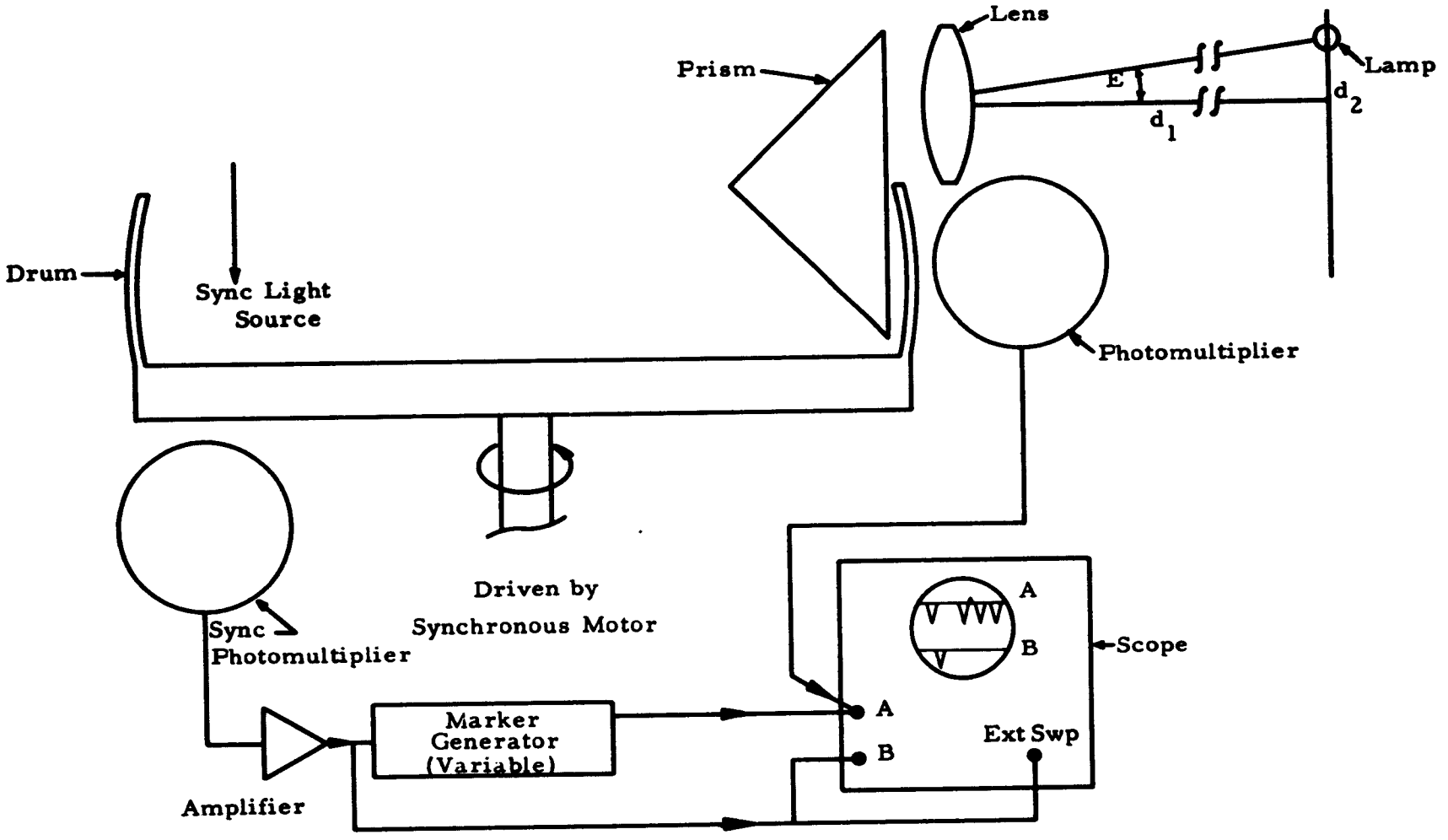

ELECTRONIC SETUP FOR DYNAMIC MEASURE OF ELEVATION ACCURACY OF PERSEAS

FIGURE 19

to be able to read the pulse position with high accuracy. Amplification of the sweep required variable reference marker on the sweep to keep up with the sweep displacement when measuring the time $P_1 - P_2$ and $P_2 - P_3$. The variable gate generator provided the marker. The marker could be set at any place on the sweep and displacement of the sweep could be very accurately measured on the scope face by counting the distance the marker had been moved.

The elevation accuracy has been presented by plotting the actual relative elevation angle vs the measured elevation angle which is,

$$\epsilon \propto \left[\frac{P_1 - P_2}{P_1 - P_3}\right]$$

Since the scope sweep is linear with time, the pulse distances are directly proportional to time and the distances ratio is what was actually plotted.

In obtaining the elevation accuracy data, it was important that the drum velocity remain constant and this was provided by the 1800-rpm synchronous motor.

Figure 20 is a plot of the actual elevation angle vs the measured angle for one set of the data. It can be seen that errors are within about one milliradian.

In obtaining the elevation data, the oscilloscope presentation was of all azimuth and elevation slits. With a magnified sweep display, it was possible to measure the maximum frame-to-frame pulse dispersion for a fixed light source. This displacement represents the system error due to imperfections in construction of the drum and milling of the slits. It was observed that the maximum dispersion of the pulses was about 5 microseconds. With a 1769 microsecond data frame and a field of view of about 800 mils this figures to be about 2.25 mils error. Most of the error is in the machining of the synchronization slits, and this error can be reduced to near zero with more accurate machining. Calibration should also be able to remove a large portion of this error due to variations from one slit grouping to another, as these effects repeat themselves.

Angular Coverage. - The lens used in the system has a diameter of 1 inch and a focal length of 3 inches. Displacement of the image from the central axis of the lens by more than ± 15/32 inch would cause some of the light to miss the cathode of the photomultiplier because the total length of the cathode is only 15/16 inch. From these dimensions

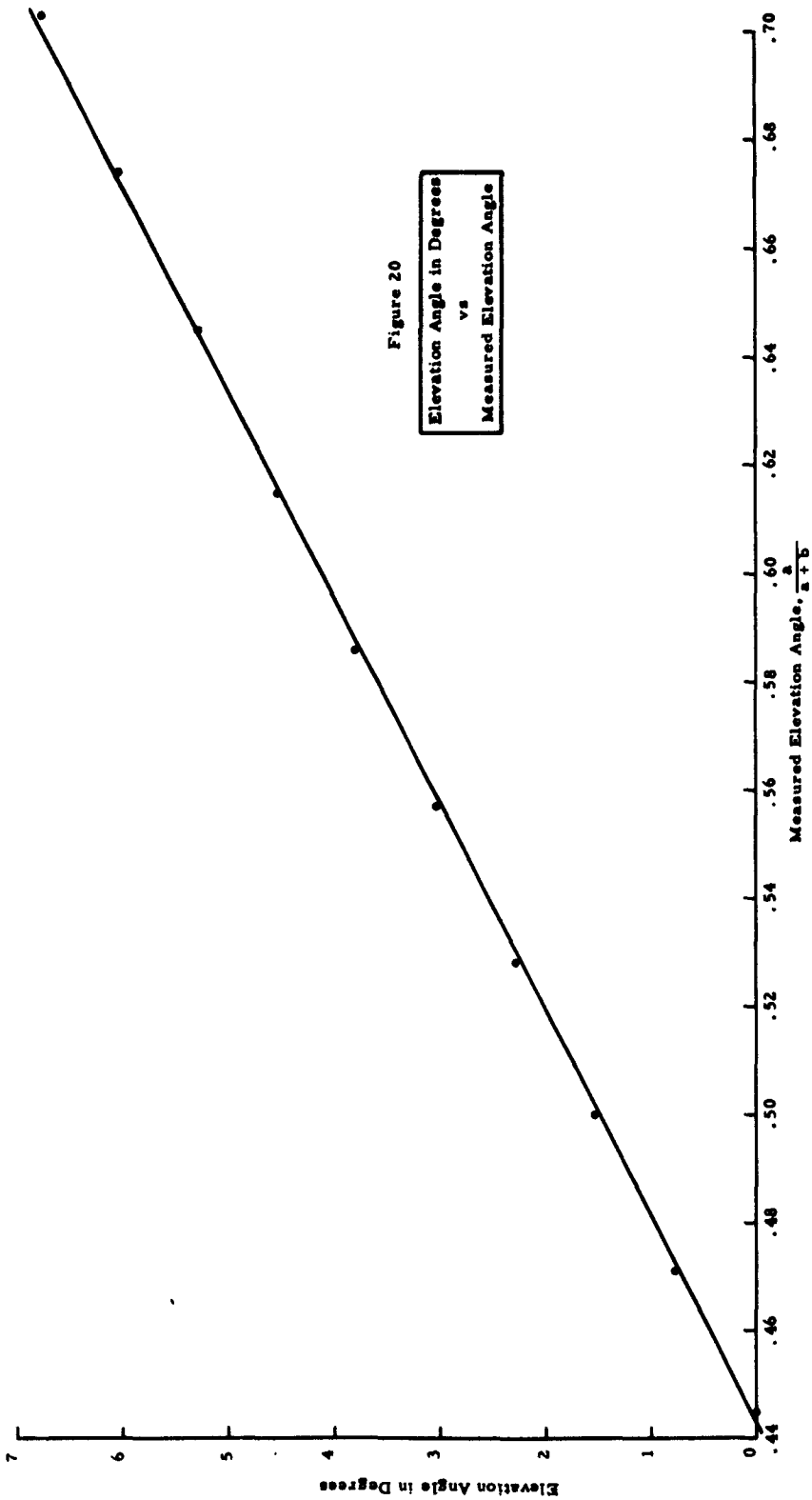

Figure 20

Elevation Angle in Degrees
vs
Measured Elevation Angle

the total angular coverage is in the order of

$$\theta_A \simeq \tan^{-1} \frac{15/16}{3} \simeq 17.5^{\circ}$$

In the Laboratory it was found with the 931A tube that about 16° was all that could be covered in azimuth. Beyond this the signal level fell off sharply. It should be noted here that the focal length of the lens is slightly increased over 3 inches by the prism and also that the photo cathode surface is slightly beyond the focal point. The rotating drum is placed as near the focal point as possible and the envelope of the photomultiplier tube is about 1/16 inch beyond the outer drum surface. The cathode of the 931 is within the envelope about 1/4 inch. From these figures it is seen that the photo cathode surface is about 3/8 inch beyond the focal point.

The angular coverage in elevation is less than the azimuth coverage. This difference is not due to the lens, prism, or the slits. The 931A photo cathode is only 5/16 inch wide and this orientation is used in the elevation plane. With this dimension it is seen that the maximum elevation angle coverage is in the order of

$$\theta_E \simeq \tan^{-1} \frac{5/16}{3} = 6^{\circ}$$

Measurements at angles slightly greater than this were permitted, however, because of the photo cathode being beyond the focal point.

It is clear from calculations and measurements made that the angular coverage is being limited by the photomultiplier. In a more refined model of the PERSEAS it will be necessary to design the system to provide an optical path between the slits and the photomultiplier such that all light passed through the slits will reach the photo cathode and the coverage angle will not be limited by the location of the photo cathode. A bundle of optical fibers from the slits to the cathode could be a solution to this problem. Another technique has been tried which uses a plastic "light funnel" covered with silver leaf to reflect the light rays and contain the light in the funnel. This technique works very well. Angular coverage in both azimuth and elevation has been increased to the limit of the optics using this technique. Azimuth coverage was measured to be about 35° and elevation coverage about 16°. This technique also allows placement of the photomultiplier in a convenient place away from the rotating drum.

Outside Operation in Conditions of Daylight and Darkness. - PERSEAS was operated outside in the daytime and at night to obtain information about the signal-to-noise ratio for different filters and

for various light sources. The information was obtained using the 1P21 photomultiplier tube. The 4730 Angstrom filter was used after it was determined there was not much difference between it and the 5380 Angstrom filter. The following sources for light were used:

1. 1000-watt input Xenon lamp
2. 11" diameter silver sphere
3. Various size mirrors
4. Odd-shaped aluminum plates
5. White surface

In the daytime on a sunny day the 1000-watt lamp can be detected with a favorable signal-to-noise ratio out to about 100 feet. After dark this distance goes up to about 1000 feet. Indications are that with a Mercury Xenon lamp of the same type and a different filter the daytime signal-to-noise ratio can be improved by a factor of about 10. This is due to a Mercury spectral line in the green region of the spectrum. Figure 24 is a photograph of the Xenon lamp which was used in the studies. This lamp operates on about 60 volts d.c., and it requires a high voltage radio frequency source to start it. It is a model 538C9 manufactured by Hanovia, Inc. For scoring problems in which the background is dark, this lamp or the Xenon-Mercury lamp would make an excellent source.

An 11-inch silvered sphere was used as a passive source during the daytime to reflect sunlight into the PERSEAS. Since the surface is spherical, only a small area is reflecting light into the system, and the maximum distance at which it could be detected was only about 50 feet. The subject of reflecting spherical surfaces will be treated in the final report on the basic contract and will not be covered here; however, it should be stated here that larger reflecting spheres appear to be promising as passive radiant sources and emphasis is not being placed on active radiant sources as a requirement for the system.

Various size mirrors were used to reflect sunlight into the PERSEAS. The results of these experiments were very encouraging in that very good signal-to-noise ratios could be obtained at long distances during daylight conditions when the background noise level was at a maximum. Mirrors from 1/256th square inch to 1/4th square inch were used to reflect light into the system. A very good signal-to-noise ratio was obtained with the 1/256th square inch mirror at a range of 250 ft, and with a 1/4th square inch mirror a very good signal was readible at about 900 ft. It is not known how distant the 1/4th inch mirror could have been taken and still provided a good signal. Studies with the mirrors have led to the consideration

of using small flat mirrors on a spherical surface to make a passive radiant source. Although time will not permit experiments with this idea it can be stated that the concept is promising.

Some studies were made using odd-shaped aluminum plates as reflectors of sunlight. As expected, the plate alignments which produced specularly reflected sunlight at the lens resulted in a strong signal. With other plate orientations only diffuse reflections (scattered light) were received and produced no detectable signal.

During observation of reflective surfaces it was noted that white materials were fairly well detected. For example, a person's white shirt would produce a detectable signal out to about 50 feet.

Quantitative studies of reflective sources were not made. This would have taken additional electronic instrumentation and consumed more time than was available. These studies which were made were primarily to get a feeling for background noise and signal intensity for sources that were available.

Photographs. - Some photographs of the PERSEAS experimental system and associated test facilities have been made. They are:

1. Figure 21, Experimental PERSEAS System with Front cover Removed
2. Figure 22, Rotating Drum of PERSEAS
3. Figure 23, Lens and Prism of PERSEAS
4. Figure 24, Xenon Lamp
5. Figure 25, Zirconium Lamp with Red Filter
6. Figure 26, Laboratory Setup for PERSEAS Studies
7. Figure 27, Experimental Setup for Outside Studies of PERSEAS

Drawings

1. Figure 28, Photomultiplier Circuit
2. Figure 29, Power Supply for Photomultiplier

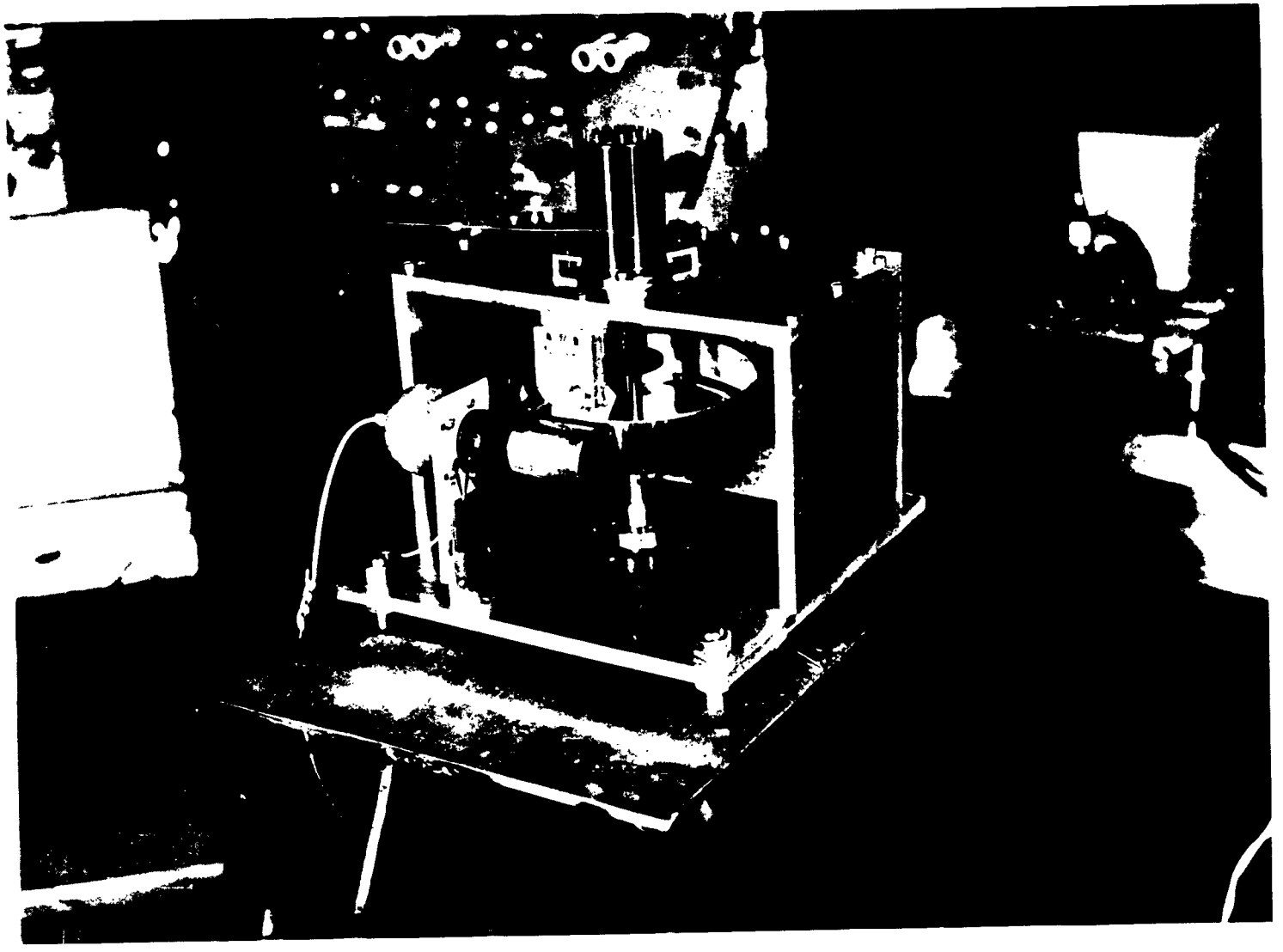

Figure 21, Experimental PERSEAS system with Front Covered Removed

Figure 22, Rotating Drum of PERSEAS

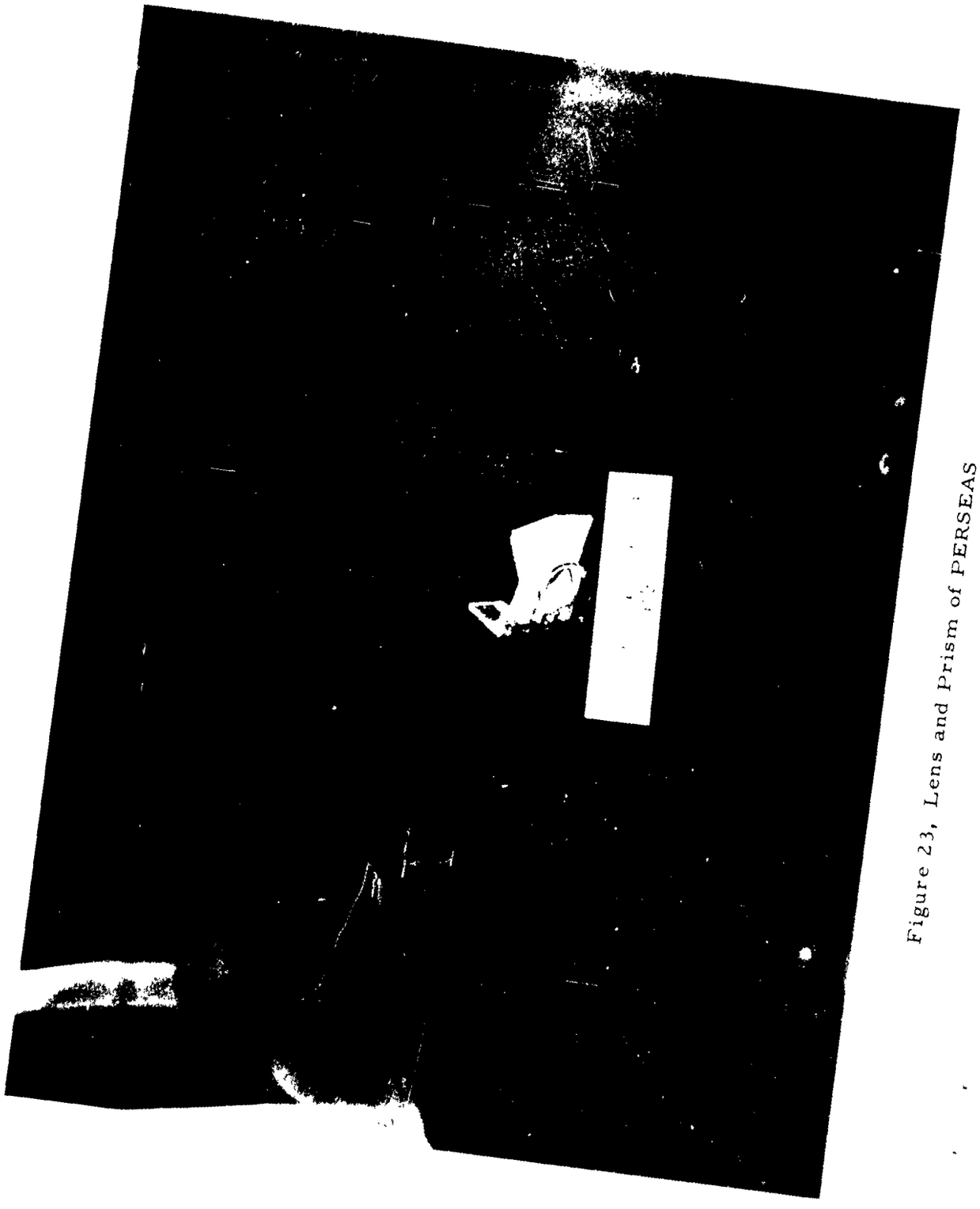

Figure 23, Lens and Prism of PERSEAS

Figure 24, Xenon Lamp

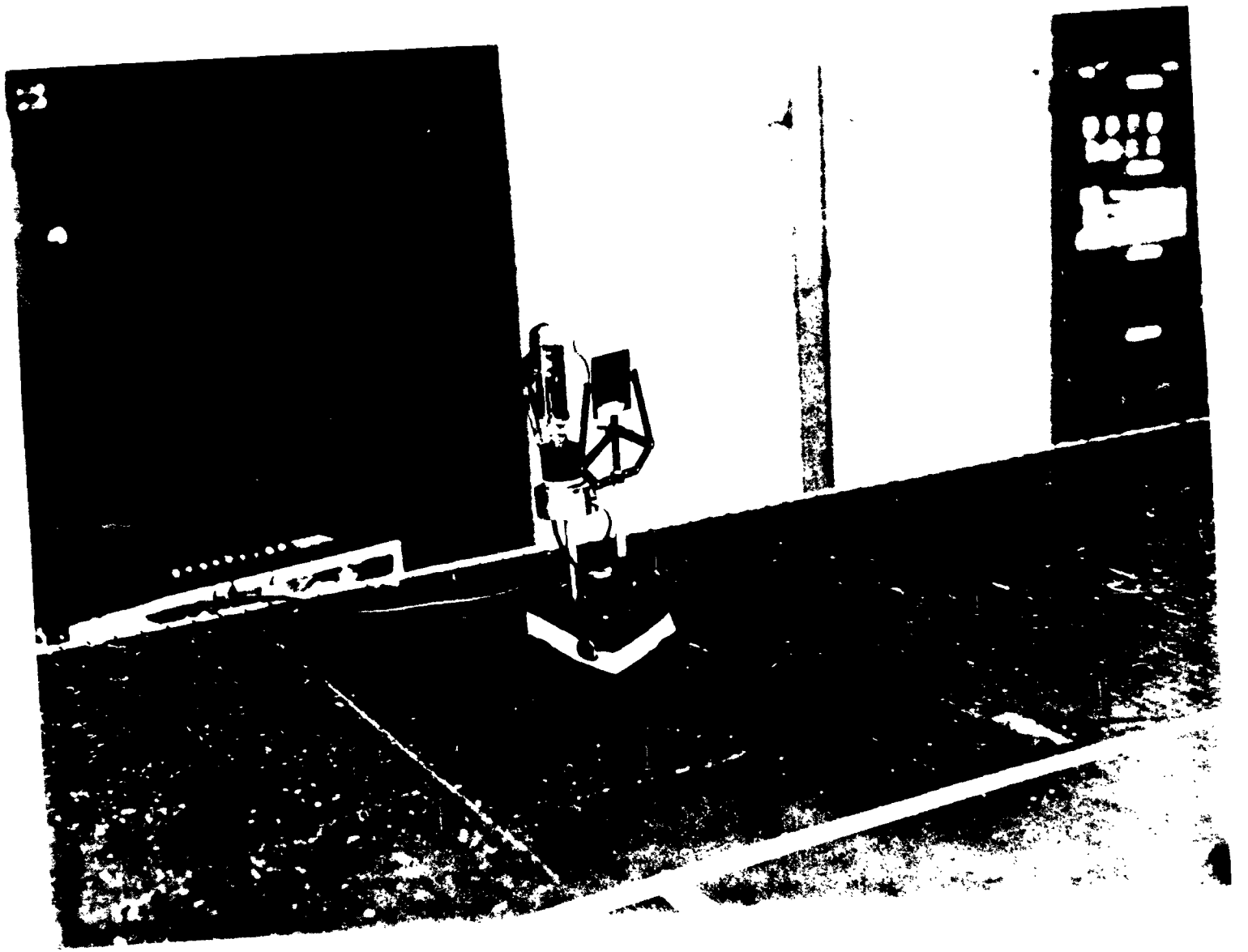

Figure 25, Zirconium Lamp with Red Filter

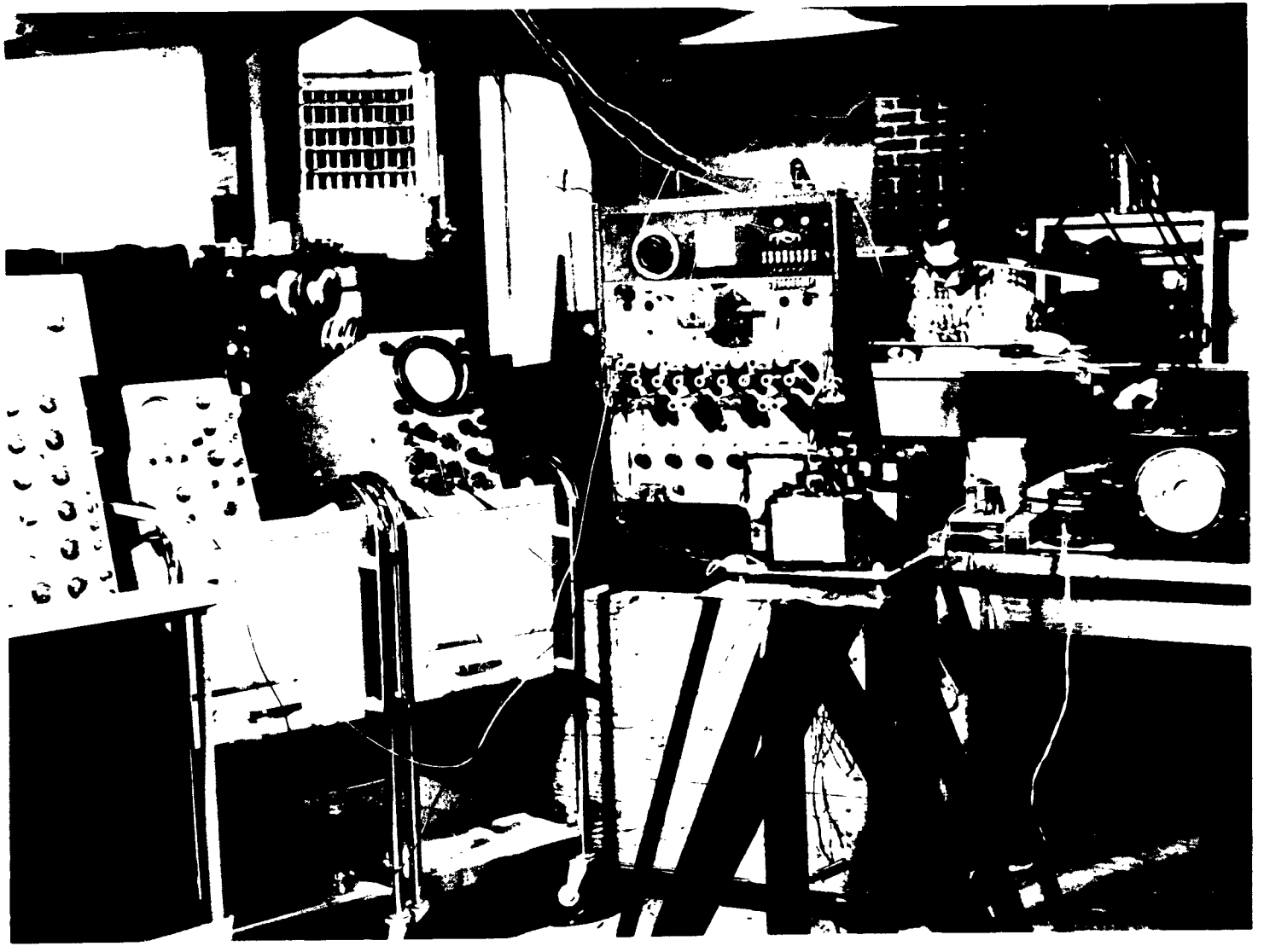

Figure 26, Laboratory Setup for PERSEAS Studies

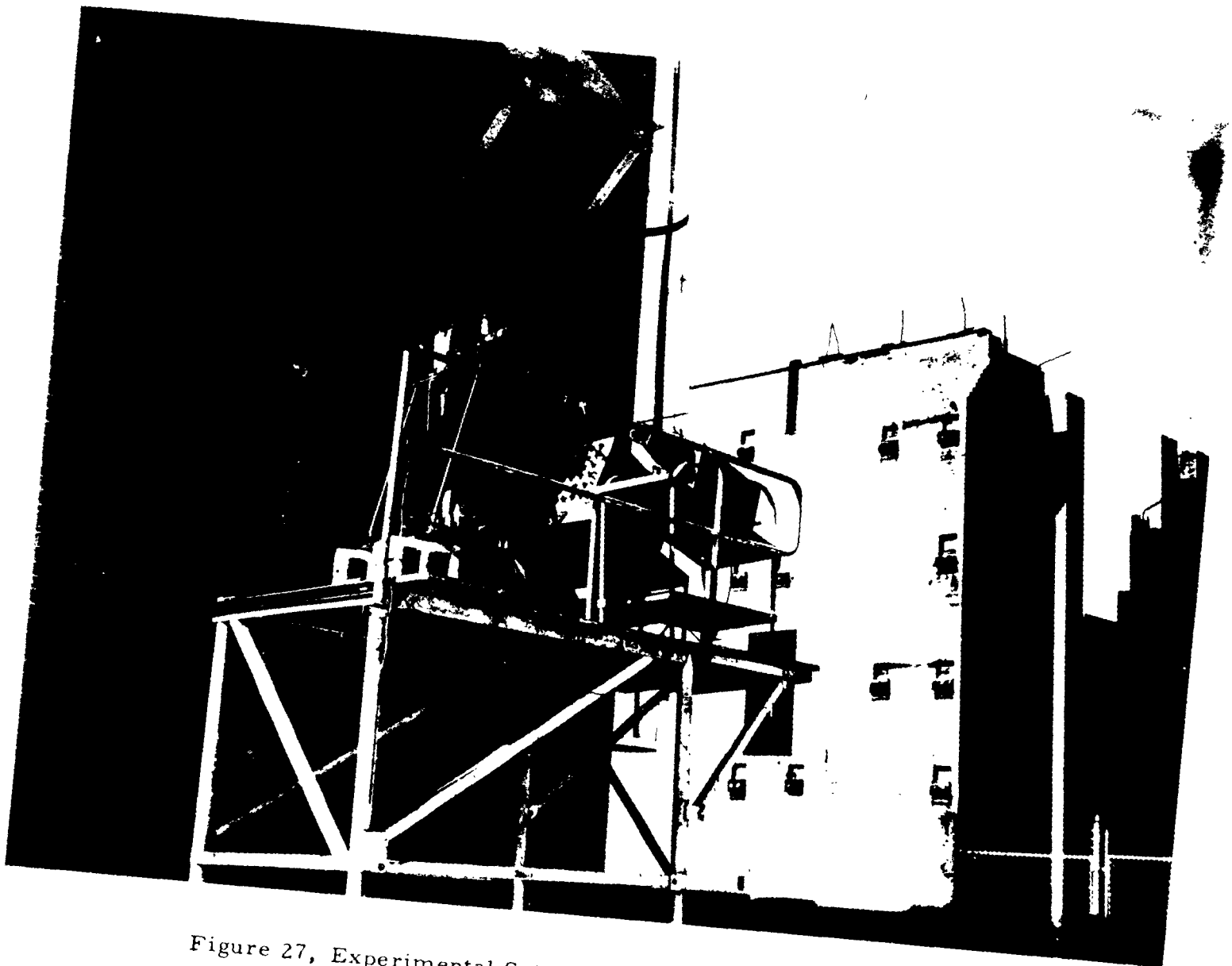

Figure 27, Experimental Setup for Outside Studies of PERSEAS

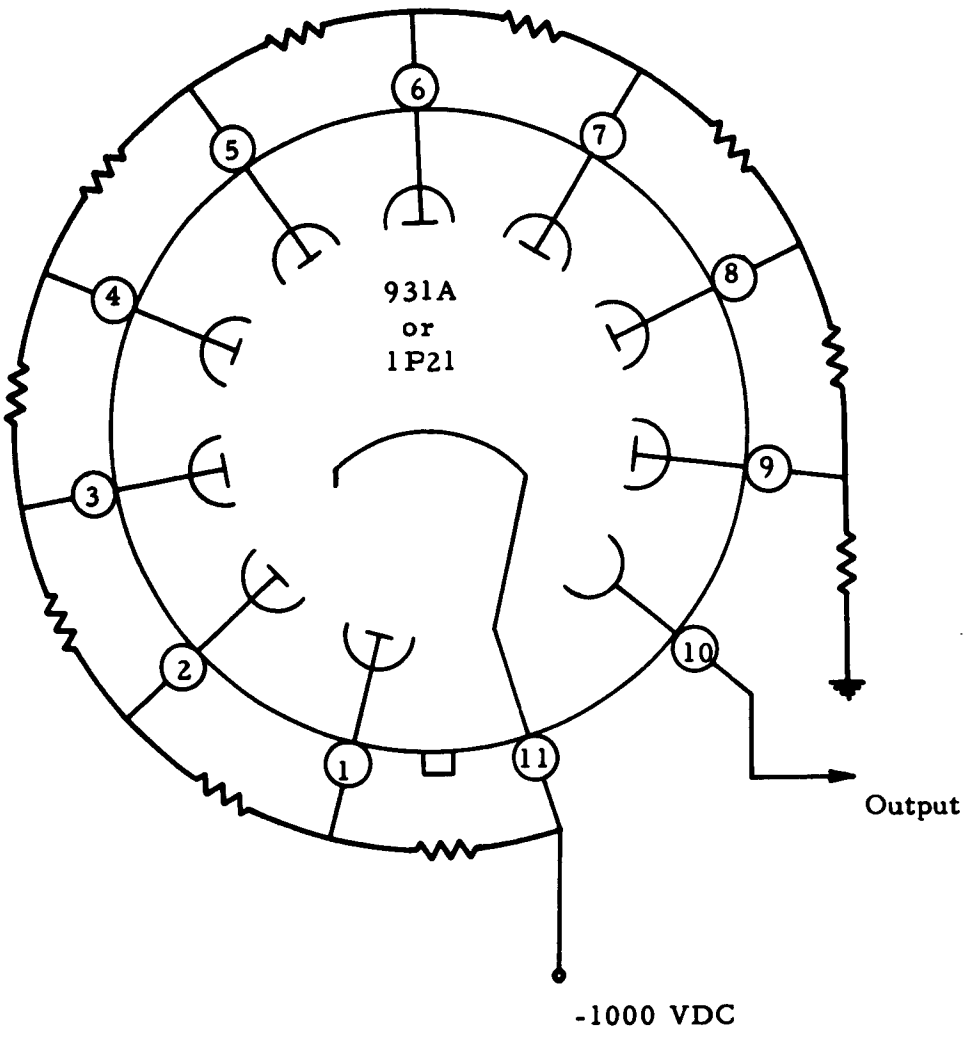

All Resistors
100,000 Ohms
1/2 Watt, 1%

PHOTOMULTIPLIER CIRCUIT

Figure 28

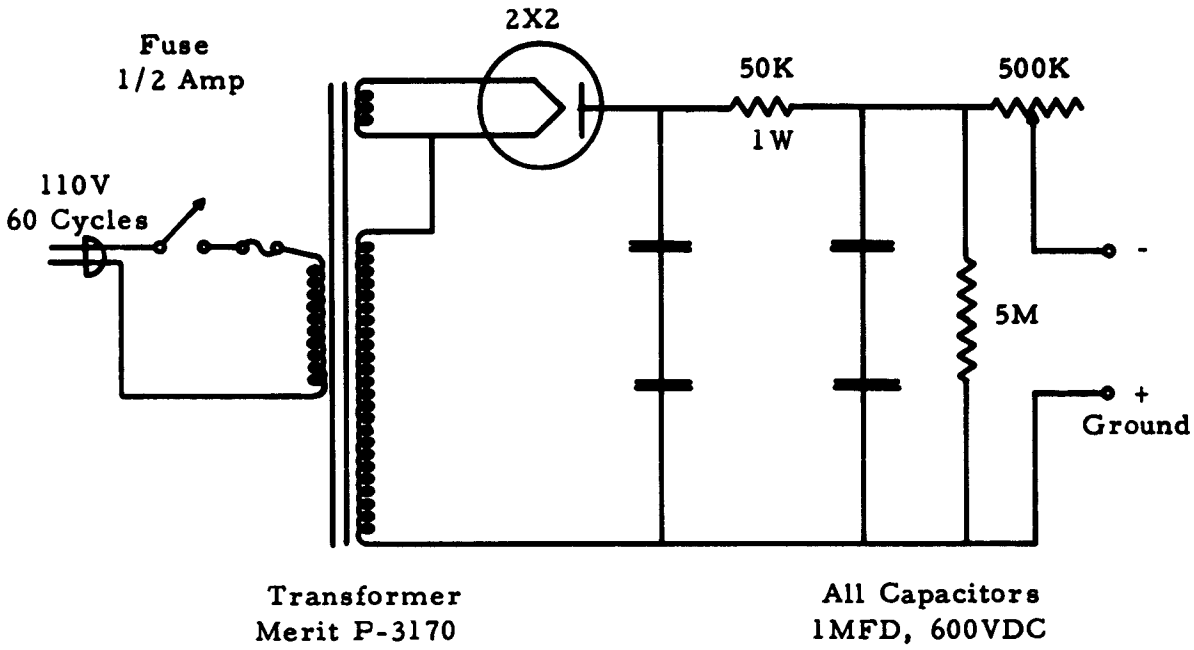

PHOTOMULTIPLIER
POWER SUPPLY

Figure 29

VI. CONCLUSIONS

From the feasibility studies of the PERSEAS system, it has been concluded that the concept has the basic desirable features needed for the design of a scoring system. This conclusion has been reached because it has been demonstrated that the device;

1. Has the required angular accuracy
2. Has sufficient sensitivity
3. Has required response time
4. Can be engineered for all angle coverage.

There are problems associated with the concept. The foremost problem is that of finding a light source which will maximize the signal-to-noise ratio but which will still be compatible for purposes of augmenting a munition to be scored. It is much more desirable, however, to have available a scoring system which is sensitive enough to "see" the munition to be scored by sensing radiation reflected from it. It appears possible that optimization of the PERSEAS system will enable the scoring of reflective vehicles. Methods of optimization would include:

1. Wavelength selection
2. Light polarization
3. Selection of reflective materials
4. Physical arrangement of reflective materials
5. Selection of wavelengths which are absorbed in earth atmosphere
6. Selection of wavelengths which are absorbed by the earth

It is further concluded that the PERSEAS system has proved successful enough to justify additional effort for perfection of the concept.

VII. RECOMMENDATIONS

It is recommended that additional effort be placed on the PERSEAS system with the following objectives for the work.

1. Design an optimum optical system which will maximize the signal-to-noise ratio.

2. Design a combined optical and photomultiplier system which will direct the received light onto the photoelectric cathodes for all incident angles.

3. Design and fabricate the system for 360 degree azimuth coverage and 60 to 90 degree elevation coverage. Minimize weight and volume to the maximum extent.

4. Design and fabricate an electronic system for the photomultiplier signals, consisting of power supplies, photomultiplier amplifiers, frequency discrimination circuits and other associated circuitry.

5. Determine specifications for a telemetering system for the device for transmission of all data. It should be an IRIG telemetry system.

6. Design and fabricate a minimum inertia rotating-slit system for the angular coverage specified. Integrate the drive motor with the optics and electronics for minimum volume.

7. Design and fabricate mechanical elements to secure the optical components and allow for precise adjustment of each component.

8. Develop a technique for the precise adjustment and calibration of the entire optical system.

9. Design and fabricate a minimum-volume enclosure for the entire system.

10. Conduct tests to determine the overall performance characteristics of the system.

    a. Determine maximum range for active and passive targets (1000 yard range is considered good).

    b. Determine azimuth and elevation errors throughout the field of view (2 mil accuracy is considered good).

c. Determine the telemetry system requirements.

11. Fabricate an additional system and determine its accuracy.

12. Combine the two systems on a base line of 2 to 5 feet. Obtain performance data from a target whose relative coordinates are well known. Compare the system's trajectory data to the known trajectory. Range errors should not exceed 10% or 50 ft (whichever is greater applies).

13. All systems for determining relative range vectors must have a method for determining the required relative angular coordinates. The feasibility of determining these angles to a high degree of accuracy with the PERSEAS concept has been demonstrated. Use of triangulation from multiple observations thus affords a solution to the scoring problems. It is recommended that further studies be made to explore the possibilities of extending the concept to integrate a method of directly obtaining a scalar range.

14. Conduct experimental and theoretical studies to determine techniques for maximizing signal-to-noise ratio.

REFERENCES

1. Adjustment and Triangulation of Fixed Camera Observations, Duane Brown, BRL Report No. 960, Ballistics Research Laboratories, Aberdeen Proving Ground, Maryland, October, 1955, (Appendix C).

2. RCA Photosensitive Devices and Cathode-Ray Tubes, Radio Corporation of America, Electron Tube Division, Harrison, N. J.

3. Amperex Tentative Data, 150 CVP Photomultiplier, Amperex Electronic Corporation, Hicksville L.I., N.Y., January 1962.

INITIAL DISTRIBUTION

1	Hq USAF(AFRDR)
2	SSD(SSTRG/TAM, 730F)
4	SSD(SSPSD)
2	SSD(SSPRS)
2	ASD(ASRNGE-2)
2	ASD(ASRSM)
3	ASD(ASAPT)
2	RTD
1	AU(AUL-9764)
6	Military Physics Rsch Lab
15	DDC
	APGC
	2 PGAPI
	50 ASQTR

Det 4, Aeronautical Systems Division, Eglin Air Force Base, Florida
Rpt No. ASD-TDR-63-16. THE PHOTOELECTRIC ROTATING SLIT ELEVATION AND AZIMUTH SENSOR (PERSEAS). March 1963, 67p. incl illus, 3 refs. Unclassified Report

This report describes a laboratory experimental study of two optical sensing devices which appeared to be worthy of feasibility studies for the specific development of scoring devices. The first device, known as the Photopot System, did not prove feasible as a useful sensor because of its slow response and low sensitivity. The second device, known as PERSEAS is considered appropriate for futher development. Studies have shown that PERSEAS is highly accurate for the measurement of relative azimuth and elevation angles, and studies of the concept have so far revealed no major limitation which would prevent development of a complete scoring system.

1. Firing error indicators
2. Optical instruments
3. PERSEAS
I. AFSC Project 7844
II. Contract AF 08(635)-2631
III. Military Physics Research Laboratory - The University of Texas, Austin, Texas
IV. Brown, Herman E.
V. Glasgow, Mark O.
VI. Secondary Rpt No. 552
VII. In DDC collection

Det 4, Aeronautical Systems Division, Eglin Air Force Base, Florida
Rpt No. ASD-TDR-63-16. THE PHOTOELECTRIC ROTATING SLIT ELEVATION AND AZIMUTH SENSOR (PERSEAS). March 1963, 67p. incl illus, 3 refs. Unclassified Report

This report describes a laboratory experimental study of two optical sensing devices which appeared to be worthy of feasibility studies for the specific development of scoring devices. The first device, known as the Photopot System, did not prove feasible as a useful sensor because of its slow response and low sensitivity. The second device, known as PERSEAS is considered appropriate for futher development. Studies have shown that PERSEAS is highly accurate for the measurement of relative azimuth and elevation angles, and studies of the concept have so far revealed no major limitation which would prevent development of a complete scoring system.

1. Firing error indicators
2. Optical instruments
3. PERSEAS
I. AFSC Project 7844
II. Contract AF 08(635)-2631
III. Military Physics Research Laboratory - The University of Texas, Austin, Texas
IV. Brown, Herman E.
V. Glasgow, Mark O.
VI. Secondary Rpt No. 552
VII. In DDC collection

Det 4, Aeronautical Systems Division, Eglin Air Force Base, Florida
Rpt No. ASD-TDR-63-16. THE PHOTOELECTRIC ROTATING SLIT ELEVATION AND AZIMUTH SENSOR (PERSEAS). March 1963, 67p. incl illus, 3 refs. Unclassified Report

This report describes a laboratory experimental study of two optical sensing devices which appeared to be worthy of feasibility studies for the specific development of scoring devices. The first device, known as the Photopot System, did not prove feasible as a useful sensor because of its slow response and low sensitivity. The second device, known as PERSEAS is considered appropriate for futher development. Studies have shown that PERSEAS is highly accurate for the measurement of relative azimuth and elevation angles, and studies of the concept have so far revealed no major limitation which would prevent development of a complete scoring system.

1. Firing error indicators
2. Optical instruments
3. PERSEAS
I. AFSC Project 7844
II. Contract AF 08(635)-2631
III. Military Physics Research Laboratory - The University of Texas, Austin, Texas
IV. Brown, Herman E.
V. Glasgow, Mark O.
VI. Secondary Rpt No. 552
VII. In DDC collection

Det 4, Aeronautical Systems Division, Eglin Air Force Base, Florida
Rpt No. ASD-TDR-63-16. THE PHOTOELECTRIC ROTATING SLIT ELEVATION AND AZIMUTH SENSOR (PERSEAS). March 1963, 67p. incl illus, 3 refs. Unclassified Report

This report describes a laboratory experimental study of two optical sensing devices which appeared to be worthy of feasibility studies for the specific development of scoring devices. The first device, known as the Photopot System, did not prove feasible as a useful sensor because of its slow response and low sensitivity. The second device, known as PERSEAS is considered appropriate for futher development. Studies have shown that PERSEAS is highly accurate for the measurement of relative azimuth and elevation angles, and studies of the concept have so far revealed no major limitation which would prevent development of a complete scoring system.

1. Firing error indicators
2. Optical instruments
3. PERSEAS
I. AFSC Project 7844
II. Contract AF 08(635)-2631
III. Military Physics Research Laboratory - The University of Texas, Austin, Texas
IV. Brown, Herman E.
V. Glasgow, Mark O.
VI. Secondary Rpt No. 552
VII. In DDC collection